Synthesis and Photochemical Properties of Fluorescent Metabolites Generated from Fluorinated Benzoylmenadiones in Living Cells

Nathan Trometer, Bogdan Cichocki, Quentin Chevalier, Jérémy Pécourneau, Jean-Marc Strub, Andréa Hemmerlin, Alexandre Specht, Elisabeth Davioud-Charvet, Mourad Elhabiri

Synthesis and photochemical properties of fluorescent metabolites generated from fluorinated benzoylmenadiones in living cells

Nathan Trometer,[a] Bogdan Cichocki,[a] Quentin Chevalier,[b] Jérémy Pécourneau,[a] Jean-Marc Strub,[c] Andréa Hemmerlin,[b] Alexandre Specht,[d] Elisabeth Davioud-Charvet,[a] Mourad Elhabiri,[a,*]

[a] *UMR7042 Université de Strasbourg–CNRS–UHA, Laboratoire d'Innovation Moléculaire et Applications (LIMA), Team Bio(IN)organic and Medicinal Chemistry, European School of Chemistry, Polymers and Materials (ECPM), 25 Rue Becquerel, F-67087 Strasbourg, France*

[b] *Institut de biologie moléculaire des plantes/Unité Propre de Recherche 2357, Centre National de la Recherche Scientifique-Université de Strasbourg, Strasbourg, France, F-67084*

[c] *Université de Strasbourg–CNRS UMR7178, Laboratoire de Spectrométrie de Masse BioOrganique (LSMBO), IPHC, 25 Rue Becquerel, 67087 Strasbourg, France*

[d] *Conception et Applications des Molécules Bioactives, UMR 7199 CNRS-Université de Strasbourg, Faculté de Pharmacie, 74 route du Rhin, Illkirch 67401, France*

*Corresponding author. E-mail: elhabiri@unistra.fr

Abstract

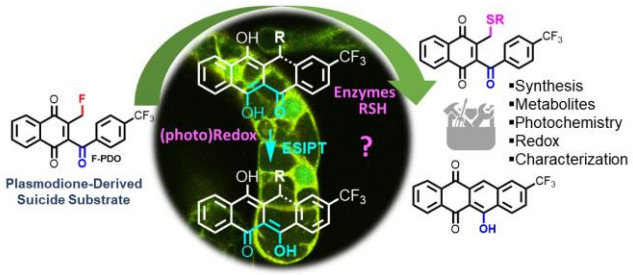

This work describes the reactivity and properties of fluorinated derivatives (**F-PD** and **F-PDO**) of plasmodione (**PD**) and its metabolite, the plasmodione oxide (**PDO**). Introduction of a fluorine atom on the 2-methyl group markedly alters the redox properties of the 1,4-naphthoquinone electrophore, making the compound highly oxidizing and particularly photoreactive. A fruitful set of analytical methods (electrochemistry, absorption and emission spectrophotometry, HRMS-ESI) have been used to highlight the products resulting from UV-photoirradiation in the absence or presence of selected nucleophiles. With **F-PDO** and in the absence of nucleophile, photoreduction generates a highly reactive *ortho*-quinone methide (*o*-QM) capable of leading to the formation of a homodimer. In the presence of thiol nucleophiles such as β-mercaptoethanol used as a model, *o*-QMs are continuously regenerated in sequential photoredox reactions generating mono- or disulfanylation products as well as various unreported sulfanyl products. Besides, these photoreduced adducts derived from **F-PDO** are characterized by a bright yellowish emission due to an ESIPT process between the dihydronaphtoquinone and benzoyl units. In order to evidence the possibility of an intramolecular coupling of the *o*-QM intermediate, a synthetic route to the corresponding anthrones is described. Tautomerization of the targeted anthrones occurs and affords highly fluorescent stable hydroxyl-anthraquinones. Although probable to explain the intense visible fluorescence emission also observed in tobacco BY-2 cells used as a cellular model, these coupling products have never been observed during the photochemical reactions performed in this study. Our data suggest that the observed ESIPT-induced fluorescence most likely corresponds to the generation of alkylated products through reduction species as demonstrated with the β-mercaptoethanol model. In conclusion, **F-PDO** thus acts as a novel (pro)-fluorescent probe for monitoring redox processes and protein alkylation in living cells.

Keywords: *Anthraquinone, ESIPT, Menadione, nucleophile, o-quinone methide, photoactivation*

Introduction

Ortho-Quinone methides (*o*-QM) are short-lived and highly reactive intermediates that are important in many processes related to organic synthesis, material sciences or medicinal chemistry.[1] Charge separation resulting from zwitterionic resonance structure stabilized by aromatic conjugation (Figure 1) lead to a reactive intermediate with a high electrophilicity of the methide carbon atom. As a consequence, *o*-QM display both a bisradical and zwitterionic character[2] and act as valuable Michael acceptors whose exo-cyclic methylene group can undergo nucleophilic addition to form benzyl adducts. In the absence of nucleophile, *o*-QM were shown to form dimers, trimers or tetramers[3] and are known to undergo facile Diels–Alder cycloadditions with various dienophiles. Among the numerous synthetic procedures, *o*-QM can be generated through thermolysis, pyrolysis, oxidation, acid-, base- or photochemical-promoted β-elimination, photolysis or enolization (Figure 1).[1,2,4-6]

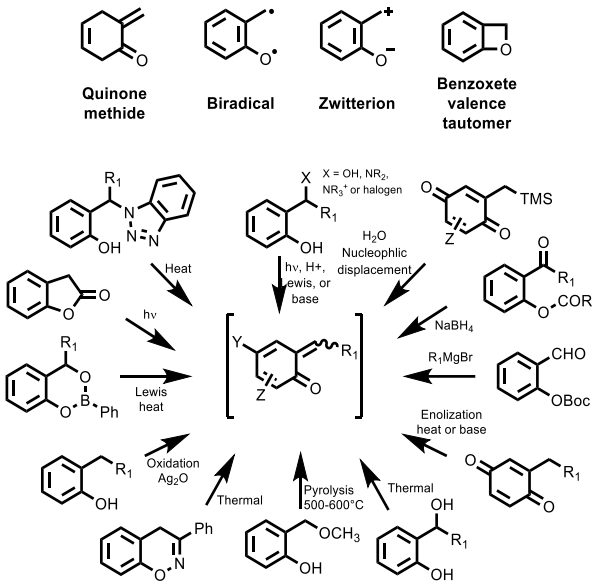

Figure 1. (Top) Possible canonical representations of *o*-QMs and (bottom) typical reactions to generate *o*-QM intermediates.

While the *o*-QM motif is present in many intermediates and products described in the literature, there are less examples of *o*-QM derived from menadione (2-methyl-1,4-naphthoquinone) or homologues and their formation often result from thermal, photochemical or basic activation (Scheme 1). For example, base-triggered enolization of 2,3-dimethyl-1,4-naphthoquinone in the presence of sodium methanethiolate (or α-toluene and *p*-toluene thiolates) results in an *o*-QM tautomer that can undergo, in the absence of oxygen, a 1,4-conjugate addition with methanethiolate to lead to a mono-sulfanylated product. Under aerobic conditions, the phenol oxidizes to the quinone, and the process repeats itself *via* a new *o*-QM intermediate to produce the *bis*-sulfanylated 1,4-naphthoquinone (Scheme 1A).[7,8] With a weakly nucleophilic base, reaction of 2-methyl-1,4-naphthoquinone derivatives, always following formation of a *o*-QM anion, were shown to afford dimeric species in the form of binaphthoquinone. Only 2,3-dimethyl-1,4-naphthoquinone led to the formation of mixture of a xanthene-type dimer and a binaphthoquinone (Scheme 1B).[9] In the menadione series, oxidation of 4-methoxy-2-methyl-1-naphthol with AgO afforded a radical species that dismutates to lead to an *o*-QM intermediate. The latter dimerizes to a spiroquinolether in a spontaneous [4+2] cycloaddition reaction (Scheme 1C).[10] The dimerization of 2-bromo-3-methyl-1,4-naphthoquinone in a tetra-*n*-butylammonium bromide ionic liquid was also completed by two successive 1,4-additions of *o*-QM intermediates and concomitant dissociation of bromide ion. The diquinone in tautomeric equilibrium with its dienol form finally leads, by oxidation, to 5,7,12,14-pentacenetetrone (Scheme 1D).[11]

Antineoplastic agents based on a substituted synthetic 6- or 2-methyl-1,4-naphthoquinone core have also been shown to generate *o*-QM alkylating intermediates after reductive activation (Scheme 1E). The most potent derivatives against ascites Sarcoma 180 cells were those substituted with mesylate, tosylate and the (chloroethyl)carbamate groups.[12] Finally, from the 6-[2'-(3'-methyl)-1',4'-naphthoquinolyl]hexanoic acid (M5) acting as a substrate of the human glutathione reductase (GR), a fluorinated analogue of 6-[2'-(3'-methyl)-1',4'-naphthoquinolyl]hexanoic acid (Fluoro-M5) was designed and investigated as a suicide-substrate (Scheme 1F). Following one- or two-electron reduction mediated by GR catalysis a highly reactive *o*-QM was generated and shown to covalently react with Cys58 of the GR active site upon fluorine elimination and thus irreversibly inactivate the enzyme.[13]

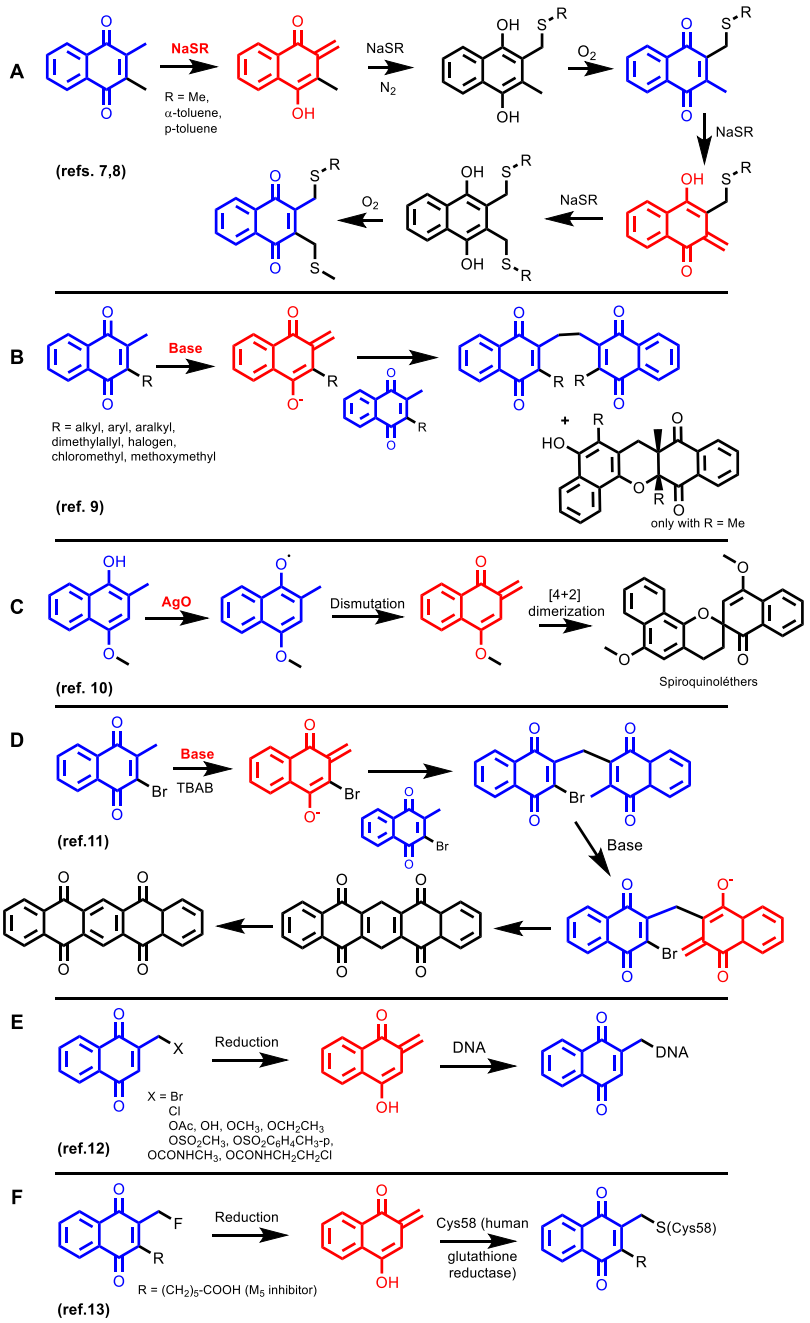

Scheme 1. *o*-QM formation and reactivity in the 1,4-naphthoquinone series for representative examples of synthetic derivatives.

For natural compounds, photochemical-induced formation of *o*-QM intermediate was also reported for 2-isoprenyl-3-methyl-1,4-naphthoquinone such as vitamin K derivatives.[14] For example, photoredox reaction of menaquinone-1 (vitamin K2) or phylloquinone (vitamin K1) leads, after 1,4-proton transfer, to a zwitterionic species that tautomerizes to a metastable isomeric *o*-QM. The latter undergoes under N_2 conditions a thermal or photochemical 6π-electro-cyclization to generate a cyclized chromenol (Scheme 2A). Under aerobic conditions, this *o*-QM intermediate can be trapped by O_2 to lead to hydroperoxide derivatives.[15] Besides, the marine natural products lomaiviticin A and B (homodimeric species) from *Polysyncraton lithostrotum* (i.e., angucycline family of aromatic polyketides) both display an uncommon diazobenzo[*b*]fluorene pattern that was also found in the kinamycins isolated from *Streptomyces murayamaensis*. Mechanistic investigations revealed that one- or two electron reductive activation of the prekinamycin biosynthetic precursor resulted in the loss of nitrogen with subsequent formation of a *o*-QM species that facilitates DNA cleavage (Scheme 2B).[16]

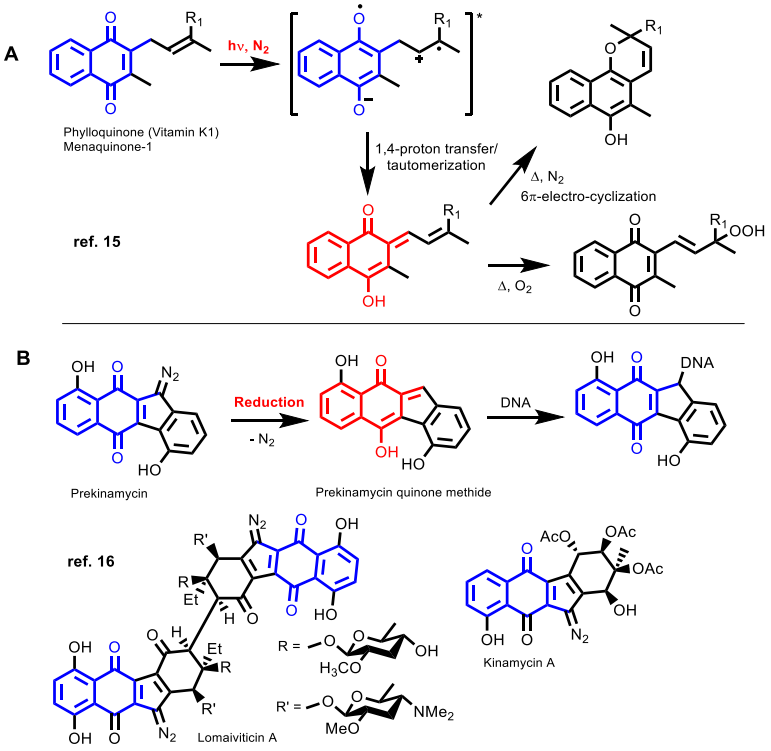

Scheme 2. *o*-QM formation and reactivity in the 1,4-naphthoquinone series for representative examples of natural compounds.

With the objective to apply the strategy used for the Fluoro-M5 derivative[13] (Scheme 1F) to the antimalarial plasmodione **PD** (Figure 1) and its **PDO** metabolite,[17] we synthesized both fluorinated analogues of **PD** and **PDO** (Figure 2). By serendipity, we discovered that the compound **F-PDO** generated an intense emission signal in tobacco BY-2 cells.[19] As the reactivity of **F-PDO** might involve a covalent labeling based on the generation of *o*-QM from a fluoromethyl-1,4-naphthoquinone subunit through biological reduction, we synthesized its potential metabolites analogues and explored thoroughly their reactivity and (photo)chemical properties. In particular, we demonstrated that activation by UV irradiation or reduction of **F-PDO** significantly favored the formation of a stable *o*-QM compared to the non-fluorinated congener. In addition, the presence of a 3-acyl residue confers to the activated species original emission properties allowing tracking their occurrence by preliminary cellular imaging studies on tobacco BY-2 cells. The alkylation of many compounds of interest for biology and in particular thiol derivatives has been monitored by various analytical methods and has evidenced, beyond the formation of original sulfanylated products, the strong capacity of **F-PDO** to act as an

efficient alkylating agent, and/or as a precursor of anthraquinones to develop into a versatile synthesis route in the future.

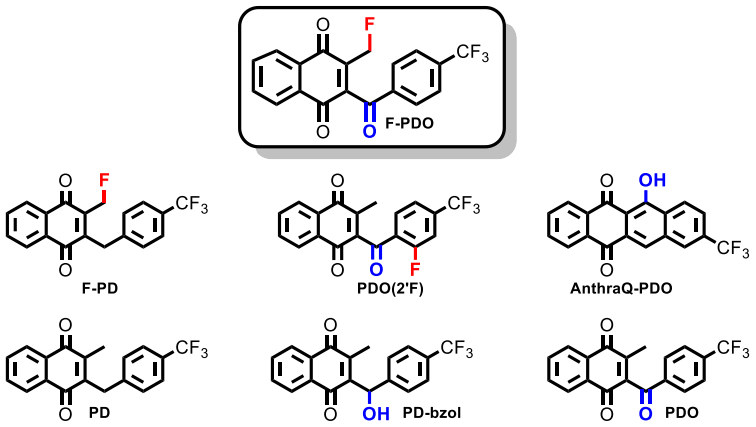

Figure 2. Chemical structures of the plasmodione derivatives investigated in this work.

Results and Discussion

Fluorescence of F-PDO in living plant cells. In a previous screening for protein prenylation inhibitors, **PD**, **PDO** and some fluorinated analogues including **F-PD**, and **F-PDO** (Figure 2) were screened using a tobacco BY-2 cell model. In this model, the expression of a fluorescent prenylation sensor (GFP-BD-CVIL protein) is regulated by and inducible promoter.[18] As reported for anthranoids[19], in this screening we employed SImaging microscopy to discriminate the fluorescence of the GFP from the putative auto-fluorescent molecules. Although none of the molecules inhibited protein prenylation, **F-PDO**-treated cells exhibited an unexpected yellow to green fluorescence, which was markedly distinct from that of the GFP-sensor. Regarding these preliminary data and to characterize accurately the fluorescence of **F-PDO** observed by SImaging, experiments were repeated without the expression of GFP. At 20 and 40 µM of **F-PDO**, a distinct and rather bright fluorescence was observed in the cytoplasm of BY-2 cells by SImaging at λ_{exc} 405 nm (λ_{405}) and λ_{exc} 488 nm (λ_{488}) excitation wavelengths, after only 5 minutes of treatment (Figure 3, Figures S1 and S2 in the ESI). The fluorescence spectra obtained at λ_{405} has a λ^{max} = 548 ± 5 nm instead of 565 ± 5 nm at λ_{488} settings (Figure 3). Moreover, another fluorescence spectrum with λ^{max} = 548 ± 5 nm was acquired only in the nucleus of cells observed at λ_{488} (Figure 3B). However, the later shape and λ^{max} was very similar to those from the fluorescence detected in the cytoplasm at λ_{405}, except that the fluorescence intensity was two times higher at λ_{488} (Figure 3, Figures S1 and S2 in the ESI). In general, for all fluorescence SImaging measurements, the absolute values of the fluorescence intensities were doubled between cells treated with 20 and 40 µM of **F-PDO**, demonstrating that concentration is not a limiting factor. Overall, these data confirmed that **F-PDO** is well absorbed by plant BY-2 cells, and leads to bright fluorescence signals from which at least two distinct emitting species could be identified by SImaging. To characterize the fluorescent species observed *in vivo*, detailed physico-chemical and photophysical investigations were first carried on **F-PDO** and compared to related derivatives in solution.

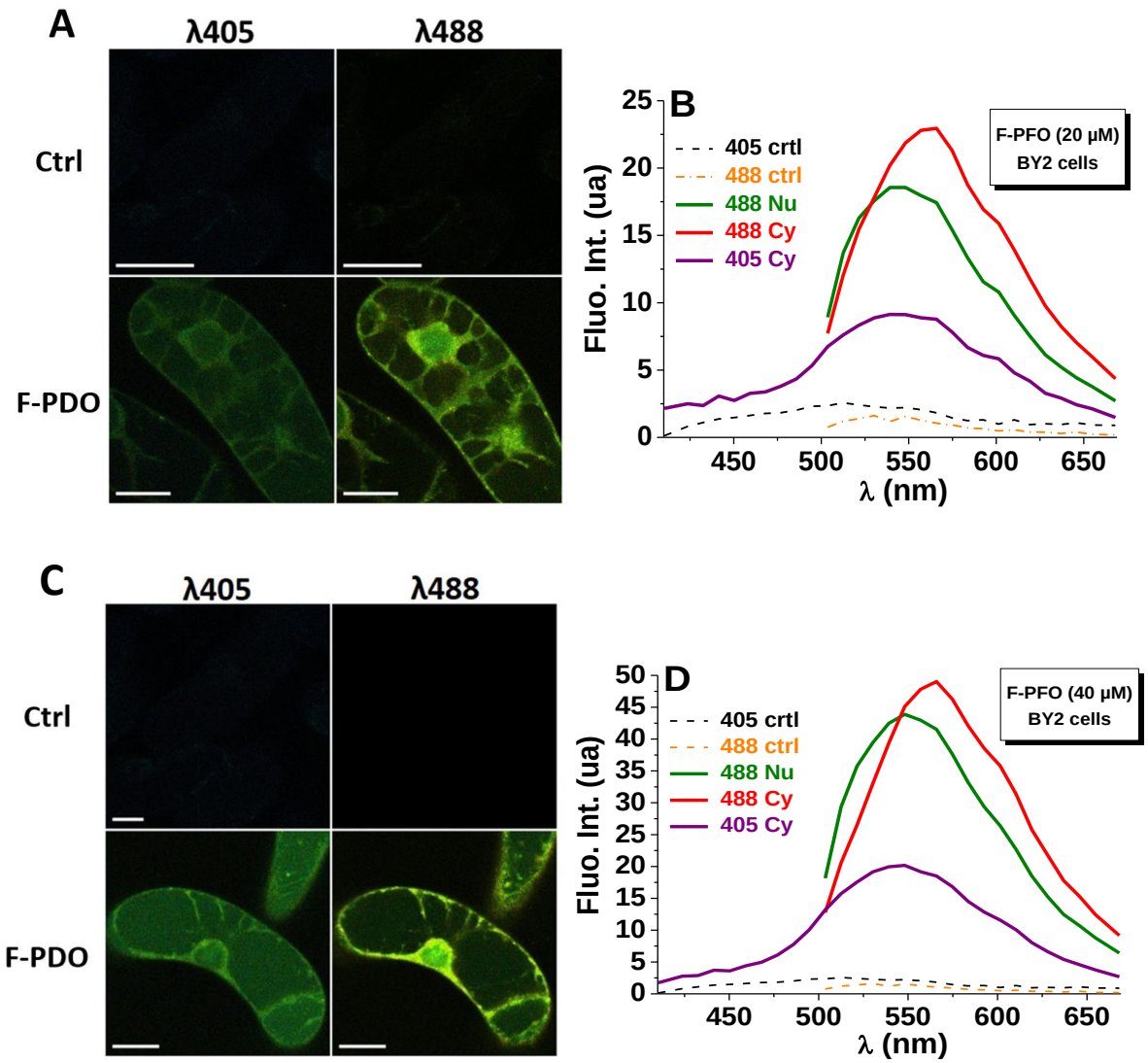

Figure 3. Fluorescence observed by SImaging in the cytoplasm (Cy) and the nucleus (Nu) of plant BY-2 cells in the presence of **F-PDO**. (Left) Images of lambda view (the bar corresponds to 20 µm) for (A) 20 µM of **F-PDO** and (C) 40 µM of **F-PDO**. Fluorescence spectra from SImaging analysis at λ_{405} and λ_{488} of BY-2 cells treated for 5 minutes with (B) 20 µM or (D) 40 µM of **F-PDO** (solid lines) compared to DMSO (Ctrl, dashed lines). These data capture the absorption of **F-PDO** within 5 min, resulting in a specific green-yellowish fluorescence as compared to the autofluorescence background illustrated by the DMSO Ctr. The presence of two distinct spectra in the cytoplasm (λ_{max} = 566 nm) and the nucleus (λ_{max} = 548 nm) suggests that at least two different species are observed under these experimental conditions.

Synthesis of 2-fluoromethylplasmodione F-PD (3) and its benzoyl derivative F-PDO (5). Based on previous works in our team,[13,20] a synthetic route has been suggested allowing the formation of compounds of interest **F-PD (3)** and **F-PDO (5)** (Scheme 3). In this section, we only report the last steps leading to **F-PD (3)** and **F-PDO (5)** starting from 2-bromo-3-(fluoromethyl)-1,4-dimethoxynaphthalene **1**. The fluorinated compound **1** could be involved in two separate routes depending on whether **F-PD (3)** or **F-PDO (5)** should be formed. **F-PD (3)** was obtained by performing a halogen-metal exchange using *n*-butyllithium on the fluorinated 1,4-dimethoxynaphthalene **1** giving the lithiated intermediate, which is then protonated in acidic media. The demethylation and oxidation of the latter was possible by using cerium (IV) ammonium nitrate (CAN) giving access to the 2-fluoromethylnaphthoquinone **2**.[13] Finally, a Kochi-Anderson benzylation, a radical alkylation, was proceeded using compound **2**,[21] the corresponding phenylacetic acid and silver nitrate/ammonium peroxodisulfate to afford the desired **F-**

PD (3). Instead of the direct protonation in acidic media after the halogen-metal exchange, compound **2** was acylated using 4-trifluoromethylbenzoyl chloride to give **4**. Finally, CAN was again used for the deprotection and oxidation of the 1,4-dimethoxynaphthalene ring enabling the access to **F-PDO (5)**.

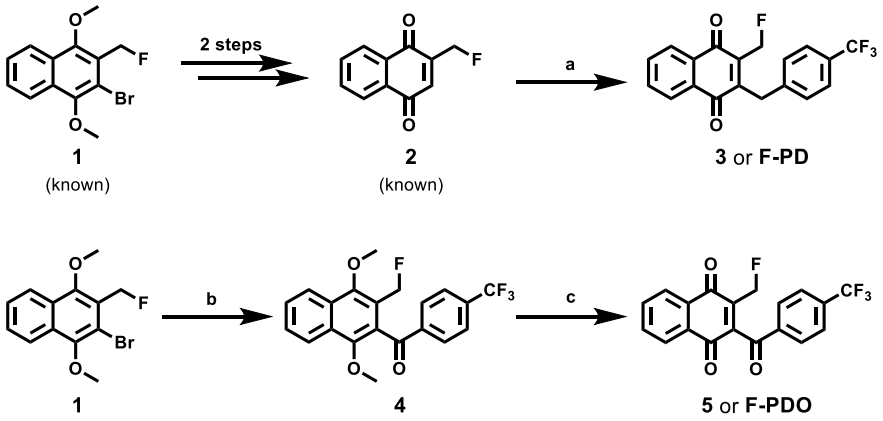

Scheme 3. Synthesis of **F-PD (3)** and **F-PDO (5)** from 2-bromo-3-(fluoromethyl)-1,4-dimethoxynaphthalene **1**. Reagents and conditions: (a) 4-(trifluoromethyl)phenylacetic acid, $(NH_4)_2S_2O_8$, $AgNO_3$, MeCN, H_2O, reflux, 3 h, 37%. (b) i. *n*-BuLi, THF, -78 °C, 10 min. ii. 4-(trifluoromethyl)benzoyl chloride, THF, -78 °C, 50 min, 83%. (c) CAN, MeCN, H_2O, r.t., 1 h, 74%.

Synthesis of the anthraquinones, AnthraQ-PDO 12a and 12b derived from a F-PDO analogue

In order to avoid the generation of two regioisomers during the intramolecular cyclization by Friedel-Crafts reaction, which would allow forming the tetracyclic scaffold, we first decided to synthesize the symmetrical benzylic precursors (compounds **7a-b**, Scheme 4) to perform the acylation reaction. The route to access the anthraquinone derived from the **F-PDO** derivative was designed in a seven-step sequence. Herein, we report the synthesis starting from 2-bromo-1,4-dimethoxy-2-(4-(trifluoromethyl)benzyl)naphthalene **7a** and 2-bromo-1,4-dimethoxy-2-(3-(trifluoromethyl)benzyl) naphthalene **7b**, (Schemes S2 and S3). Compounds **7a-b** were then treated with *n*-butyllithium to perform a halogen-metal exchange forming the lithiated intermediates, which were acylated using methyl chloroformate giving esters **8a-b**. The formed naphthoates **8a-b** underwent saponification with potassium hydroxide,[22] followed by protonation in acidic conditions to give the corresponding carboxylic acids **9a-b**. Introducing these carboxylic acid moieties at position 2 of the naphthalene ring opened access to cyclization *via* a Friedel-Crafts acylation. Based on the previous works in our team,[23] this reaction was performed using trifluoroacetic anhydride (TFAA) in the presence of small amount of triflic acid (TfOH, 0.5 equivalent). The combination of TFAA and TfOH led to the formation of a more reactive species, trifluoroacetyl triflate, which then activated the carboxylic acid by forming an acylium cation. The latter enabled the aromatic electrophilic substitution of the compounds' benzylic moiety, thus bridging both sides of the molecule and giving compounds **10a-b**. Finally, the tetracycles **10a-b** were treated with a solution of BCl_3 in the presence of TBAI affording demethylation followed by oxidation.[24] The expected trione forms **11a-b** could not be observed. In fact, it is known that under aerobic conditions, these naphthacenetrione derivatives easily tautomerize to their aryl-alcohol analogues.[25] This can be explained by the fact that not only the aromatization stabilized the molecule, but also the intramolecular hydrogen bonding between the hydroxyl and keto moiety, thus giving 6-hydroxy-8-(trifluoromethyl)tetracene-5,12-dione **12a** (**AnthraQ-PDO isomer**) and 6-hydroxy-9-(trifluoromethyl)tetracene-5,12-dione **12b** (**AnthraQ-PDO**), respectively.

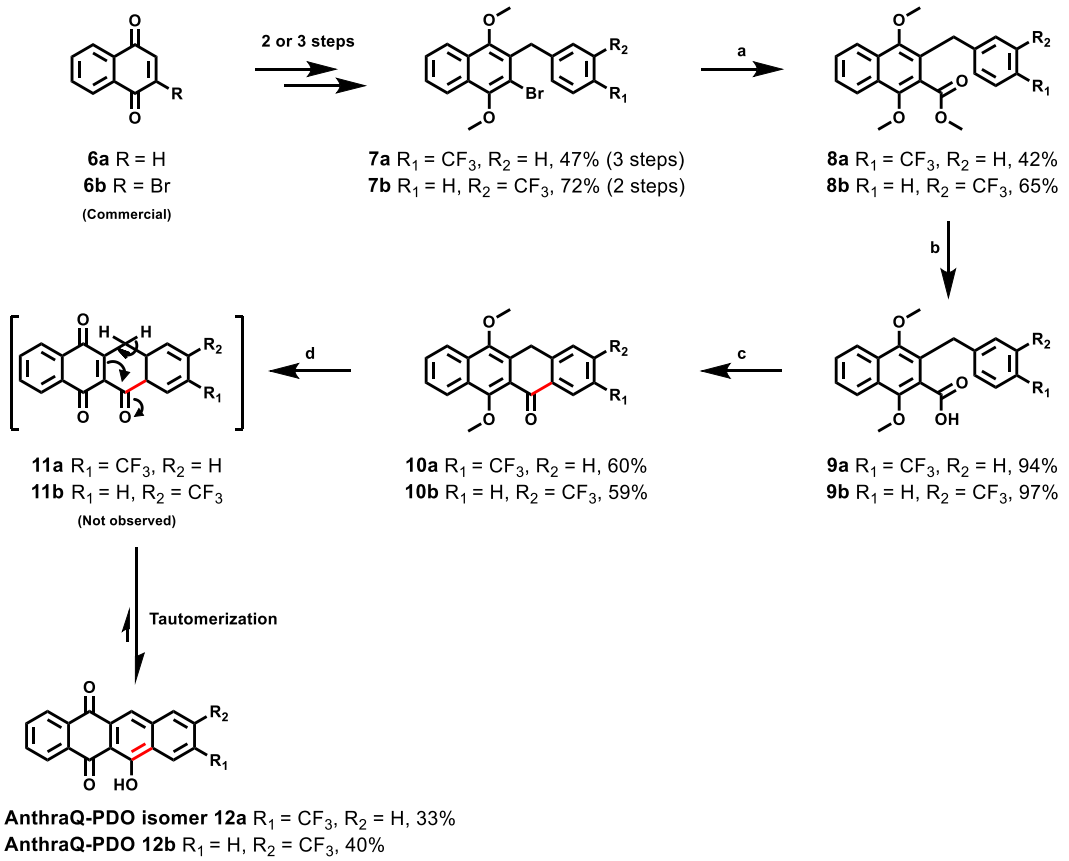

Scheme 4. Synthesis of 6-hydroxy-8-(trifluoromethyl)tetracene-5,12-dione **12a** and 6-hydroxy-9-(trifluoromethyl)tetracene-5,12-dione **12b**. Reagents and conditions: (a) i. *n*-Butyllithium, tetrahydrofuran, -78 °C, 5 min. ii. Methyl chloroformate, tetrahydrofuran, -78 °C, 1 h. (b) Potassium hydroxide, ethanol, water, reflux, 16 h. (c) Trifluoroacetic anhydride, triflic acid, dichloromethane, 0 °C to r.t., 16 h. (d) Boron trichloride, tetrabutylammonium iodide, dichloromethane, -78 °C to r.t., 16 h.

Electrochemical Properties of F-PD and F-PDO. Physicochemical studies in solution (absorption and electrochemistry) were first carried out to evaluate the reactivity of **F-PD** and **F-PDO**. The main goal was to assess the influence of photo- or electro-chemical activation on the properties of these naphthoquinone derivatives. **F-PD** and **F-PDO** were compared to their analogues **PD** and **PDO** that are lacking fluorinated substitution on the 2-methyl group of the menadione subunit. These data are also discussed with respect to those previously measured for **PD-bzol**.[17,26] Cyclic (CV) and square wave (SWV) voltammograms were first recorded in the potential range from 0 to -2.1 V *vs.* KCl(3 M)/Ag/AgCl reference electrode (+0.210 V *vs.* NHE). For **PD**, **PD-bzol** and **PDO** (i.e., **PD-bzol** and **PDO** are **PD** metabolites following **PD**'s bioactivation), we previously showed that reduction of the electroactive 1,4-naphthoquinone core resulted in two successive reversible one-electron transfers (Figures S3-S9 in the ESI) in DMSO.[27,28] The monoradical-anion, formed in the first reduction step, is reduced to its related dihydronaphthoquinone dianion in a second reduction step. **PD** was found to be the less oxidant derivative ($E^1_{1/2}$ = -0.58 V), while **PDO** is the most oxidant one ($E^1_{1/2}$ = -0.40 V). Benzylic oxidation indeed alters markedly the redox properties of the electroactive core (i.e., **PDO** is more prone to reduction than **PD**).[17,29] For **PDO**, a third redox signal at -1.58 V (Figure S5 in the ESI) is observed and was attributed to one-electron redox process centered on the benzoyl carbonyl group.[23]**PD-bzol** differs with a much stronger effect on the one-electron reduced semiquinone due to an intramolecular hydrogen bond between the benzylic alcohol and the negatively charged semiquinone subunit (Figure S7 in the ESI). By contrast, the electrochemical study conducted on **F-PD** and **F-PDO** demonstrates a strikingly different behavior (Figure 4 and Figures S4 and S6 in the ESI).

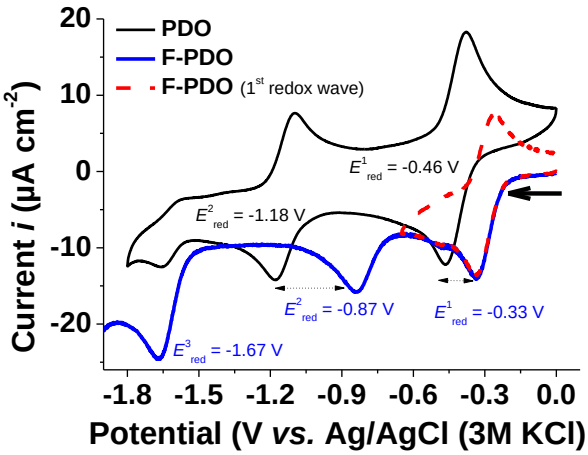

Figure 4. Comparison of the CV spectra of **F-PDO** (blue line, 1st cycle) and **PDO** (black line). Solvent: DMSO; I = 0.1 M n-Bu_4NPF_6; v = 200 mV s^{-1}; *T* = 23(1) °C. Reference electrode = KCl(3 M)/Ag/AgCl; working electrode = glassy carbon disk of 0.07 cm^2 area; auxiliary electrode = Pt wire. Starting potential = 0 V. IUPAC convention used to report the CV data. The solid arrow indicates the direction of scan.

After a first reduction cycle, a very fast chemical reaction results in an altered electrochemical behavior evolving after each redox cycle. Furthermore, a third reduction peak noticeably emerges at -1.72 V for **F-PD** (Figures S3 and S4 in the ESI). For **PDO**, a third redox wave ($E_{1/2}$ = -1.58 V, E_{red} = -1.66 V) assigned to a redox process centered on the benzoyl carbonyl group was already present (Figures S5 and S6 in the ESI). For **F-PDO**, the latter is likely merged with a new and intense reduction signal observed E_{red} = -1.67 V as seen for **F-PD**. Taken together, these data suggest that following a first one- (Scheme 5, route A) or two-electron reduction (Scheme 5, route B), **F-PD** and **F-PDO** likely undergo a fluoride F^- loss (i.e., reductive elimination) resulting in the formation of either a radical species (Scheme 5, route A) or a *o*-QM[6] (Scheme 5, route B) capable of self-associating to form a covalent dimeric species[30-32] or eventually evolving towards oligomer formation (Scheme 5). This is in agreement with related analogues such as mono-, di- and trifluoromethyl-menadiones[33] for which the presence of the fluorine atom(s) induces a significant anodic shift (> 200-340 mV) of the redox potentials of the 1st and 2nd redox waves in line with their much higher oxidant character. Following the two-electron reduction, the anions resulting from mono- and trifluoromethyl-menadiones were shown to be unstable (irreversible electron transfers) leading to formation of *o*-QM species.[33] For a deeper understanding, CV experiments were then conducted only on the first one-electron process (Figures S8 and S9 in the ESI). This signal was found to be reversible but fades (i.e., in particular for **F-PDO**) during redox cycling suggesting that the anionic monoradical (Scheme 5, route A) is likely gradually involved in the formation of the homodimeric species. The third reduction signal measured at ~ -1.7 V for **F-PD** and **F-PDO** after the first reduction sweep are likely attributed either to the reduction of the quinone methide radical[34] or to quinone methide polymerization as observed for difluoromethyl-menadione[33] and related compounds.[33,35]

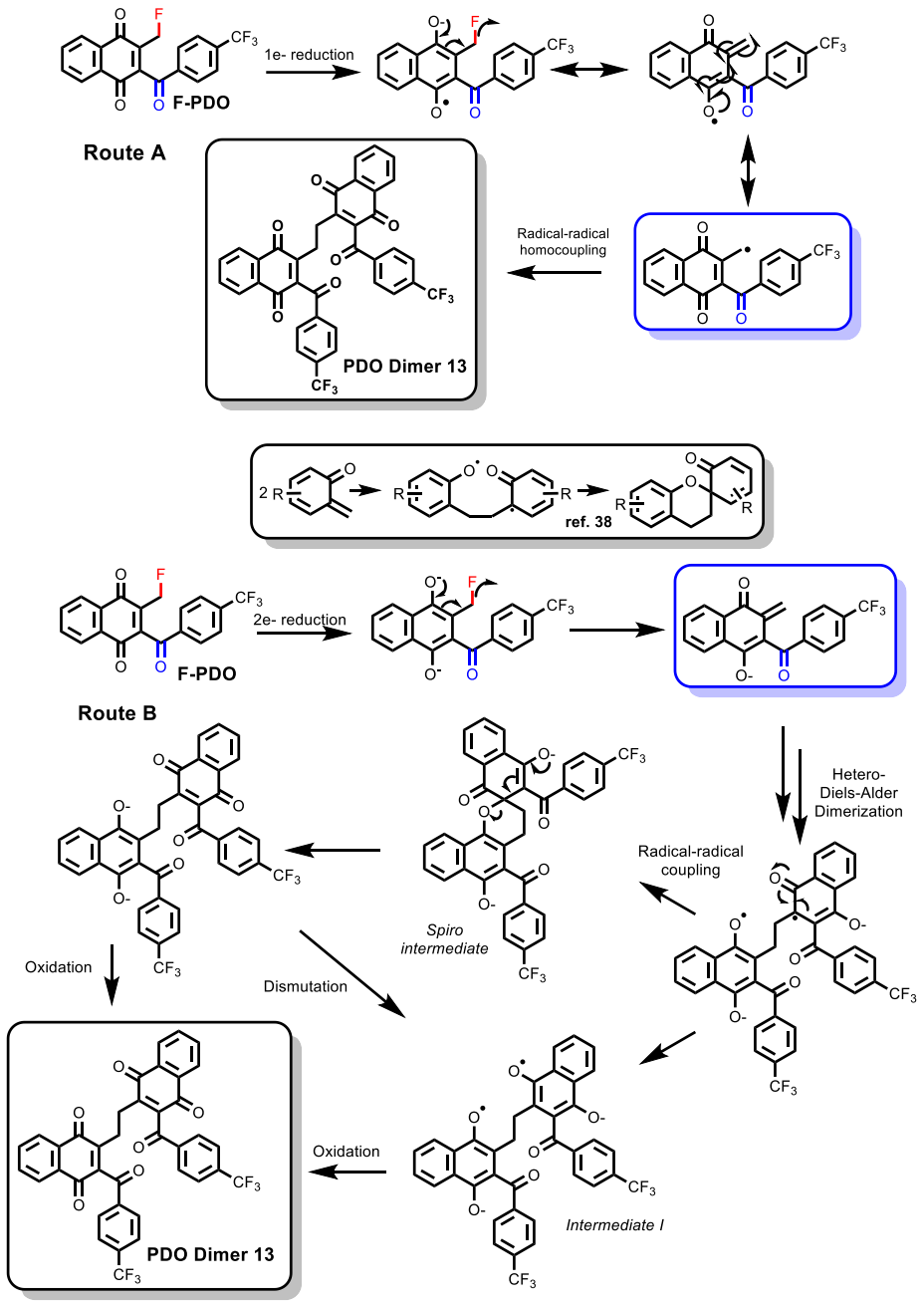

Scheme 5. Proposed electrochemical mechanisms leading to formation of the dimeric species (**PDO-dimer 13**). Route A) from the 1e- reduced species. Route B) from the 2e- reduced species.

For route A (Scheme 5), the radical species formed after the reductive elimination of F^- might spontaneously self-dimerizes (i.e., radical-radical homocoupling reaction). A heterodimeric coupling or the formation of polymeric species are unlikely to occur since this dimeric species (*vide infra*), which corresponds to the binaphthoquinone homodimer, was unambiguously characterized.[9] For route B (Scheme 5), it has been shown on related *o*-QM that a non-ionic process involving a Diels-Alder addition of two molecules can lead to spontaneous dimer formation.[10,36-38] Furthermore, *o*-QM have also been shown to undergo efficient hetero Diels–Alder reactions.[39] For a broad range of *o*-QM, radical-radical coupling was shown to lead to spiro derivatives (Scheme 5).[10,40] For **F-PD** and **F-PDO**, this spiro intermediate is most likely transformed into mixed quinone-semiquinone dimer that might undergo dismutation into a bisradical intermediate **I** (Scheme 5).[41] Whatever the electrochemical mechanism involved (Routes A or B), the homodimeric species thus seems to be the predominating

species obtained by electrochemical means. These electrochemical data agree with the closely related fluoro-M5 derivative (Scheme 1F) that was shown to act, upon one- or two-electron reduction (enzymatic catalysis and elimination of the fluorine), as a suicide substrate capable of alkylating the human glutathione reductase.[13,42]

Photochemical Reactivity of F-PD and F-PDO. UV-photoreduction of (benzo)quinones in propan-2-ol (^{i}PrOH) is known to generate among other species (e.g., dihydroquinone) semiquinone radicals.[43,44] Following UV excitation, the 1,4-naphthoquinone scaffold is photo-excited and generates an excited triplet state that can be trapped by ^{i}PrOH (i.e., H atom donor) to lead the semi-1,4-naphthoquinone radical.[45,46] In this way, UV irradiation of **PD** in ^{i}PrOH under oxygen pressure or air atmosphere allowed the benzylic oxidation to **PDO**.[17] The reactivity of **F-PDO** at 5 mM in an ^{i}PrOH/DCM (*v*/*v*) mixture was evaluated by irradiation at 350 nm for 24 h (i.e., Rayonet photochemical reactor equipped with 16 UV lamps of 14 W and maintained at 16 °C) and using high-resolution electrospray mass spectrometry (ESI-HRMS) monitoring. Absorption spectra of **F-PD**, **F-PDO**, **PD** and **PDO** measured in ^{i}PrOH/DCE (*v*/*v*) mixture first confirmed that these chromophores (π-π* transitions centered on the 1,4-naphthoquinone core at ~340 nm) are ideally suited for irradiation at 350 nm (Figure S10 in the ESI). The analysis of the ESI-HRMS spectra of **F-PDO** after 24 h of photoirradiation in ^{i}PrOH/DCM clearly demonstrates the formation of a covalent binaphthoquinone dimer (Scheme 5) as assessed by the presence of peaks at experimental *m/z* of 693.1257 ([**Dim**+Li]$^{+}$, theoretical *m/z* = 639.1324), 709.0918 ([**Dim**+Na]$^{+}$, theoretical *m/z* = 709.1062) and 725.0707 ([**Dim**+K]$^{+}$, theoretical *m/z* = 725.0801) (Figure 5A). Interestingly, the same experiment carried out in pure benzene at 5 mM by irradiation at 350 nm (Rayonet photochemical reactor) for 24 h (Figure S11 and Table S1 in the ESI) or with two crossed LED beam, a UV (365 nm) and a visible (430 nm), excitation (i.e. produced by a LUMOS 43 LED source from Atlas Photonics Inc. with a typical output of 200 mW.cm^{-2}) for 3 h (Figure S12 and Table S2 in the ESI) demonstrates the absence of reactivity of **F-PDO** and thus of dimer formation as exemplified by the presence of characteristic peaks of **F-PDO**. This feature clearly supports the essential role of H donor in the activation of **F-PDO**[45] and the importance of the semiquinone radical in the formation of the covalent homodimeric species.

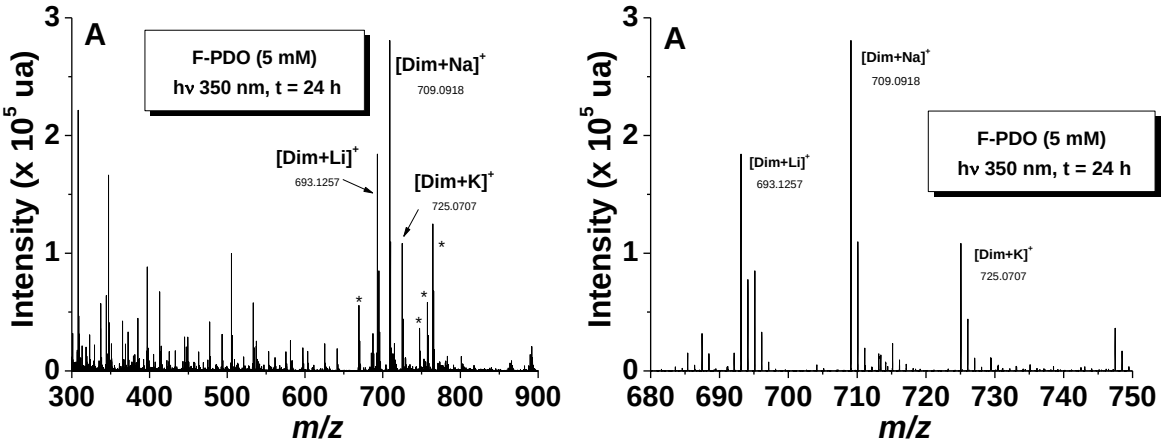

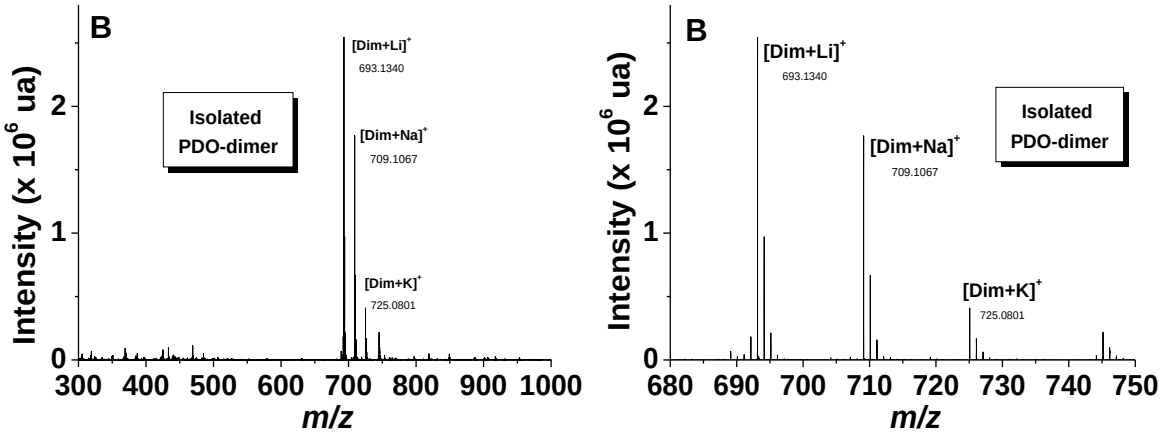

Figure 5. High Resolution electrospray mass spectra of (A) 5 mM solution of **F-PDO** after irradiation at 350 nm during 24 h in ^{i}PrOH/DCM mixture (1:1 *v/v*) and (B) isolated and purified **PDO-dimer**. Positive mode.

However, when the reaction was carried out at higher concentration (0.1 M of **F-PDO**), only the formation of the homodimer could be observed. This one could be isolated by flash chromatography on silica gel affording an orange solid, presenting no fluorescence emission. The structure of the isolated product (**PDO-dimer 13**) has been solved using ^{1}H, ^{13}C and ^{19}F NMR (see the corresponding spectra in the ESI). Using ^{1}H and ^{13}C NMR, the observed structure was shown to be symmetrical with a methylene signal at 2.77 ppm. In addition, the characteristic doublet of -CH_2F at 5.52 ppm (J = 46.3 Hz) was no longer present in ^{1}H NMR. This could be further confirmed in ^{19}F NMR showing the disappearance of the triplet at -223.16 ppm (J = 46.4 Hz), thus confirming the fluorine's elimination. Finally, ESI-HRMS analysis (ESI+, Figure 5A) showed three cationic peaks corresponding to [**Dim**+Li]$^{+}$ (*m/z* = 693.1309), [**Dim**+Na]$^{+}$ (*m/z* = 709.1046) and [**Dim**+K]$^{+}$ (*m/z* = 725.0785), respectively, thus assessing the homodimer formation under these experimental conditions.

Emission Properties under Quasi-Physiological Conditions. In order to get a deeper insight into the origin of the peculiar emission signals observed in the SImaging study of **F-PDO** in tobacco BY-2 cells, we screened the reactivity of **F-PDO**, **F-PD**, **PD** and **PDO** using a hybrid absorption/emission plate reader and under quasi-physiological conditions in the presence of different biological relevant molecules (mercaptoethanol β-met, cysteine Cys, glutathione GSH, lysine Lys, histidine His, human glutathione reductase hGR or Bovine Serum Albumin BSA) after irradiation or not at 350 nm (Rayonet photochemical reactor 224 W) for 2 h and under argon or air atmosphere. Figure 6 first shows the results obtained with **F-PDO** with mercaptoethanol β-met (R-SH: pK_a = 10.14)[47] under the different conditions tested. Photoirradiation of the 1,4-naphthoquinone core in the presence of β-met clearly resulted in yellow-green emission centered at 566 nm, whereas the same reaction performed in the absence of UV-light irradiation generated no significant emission. This result perfectly agrees with the observations deduced from the cell imaging approach (emission at 566 nm in the cytoplasm, Figure 3 and Figure 6) suggesting at first glance that thiol-based compounds could react with **F-PDO**. The presence of oxygen (air atmosphere) has apparently no impact on the formation of emissive species resulting from the reaction of **F-PDO** and β-met. In addition, the measurement of the excitation spectra under the different conditions evidenced the formation of an emissive species with electronic transitions (λ^{max} = 353 and 452 nm) lying at much lower energies with respect to those of **F-PDO** (Figure S13 in the ESI, λ^{max} = 248 and 343 nm). This is also consistent with cell imaging data for which the samples were excited at 405 or 488 nm corresponding to the wavelengths that this new species with β-met absorbs. Moreover, this agrees with the absorption spectra recorded in iPrOH/DCE after UV-photoirradiation (350 nm for 2 h 15, Rayonet photochemical reactor 224 W) in the presence of β-met. These results were compared to those measured for **F-PD**, **PD** and **PDO** in the presence of β-met

(Figure S14 in the ESI) and show that the benzoyl-menadiones **PDO** and **F-PDO** are by far much more reactive under these experimental conditions (photoirradiation at 350 nm for 2 h in the presence of β-met) in relation to their much more oxidizing character.[29] Moreover the emission signature (λ^{em} ~ 570 nm) is comparable whatever the compound considered suggesting comparable adduct formation.

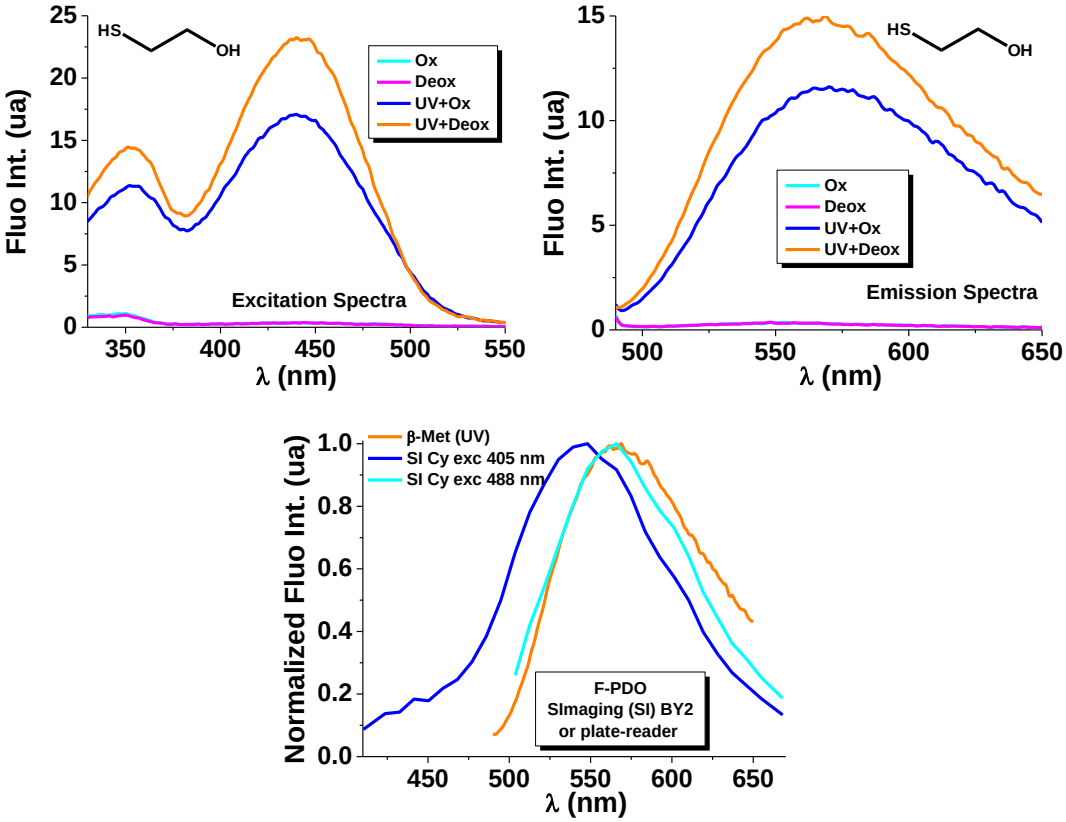

Figure 6. (Top) Excitation (left) and emission (right) spectra recorded for **F-PDO** after irradiation or not at 350 nm (Rayonet photochemical reactor 224 W) for 2 hours under argon or oxygen atmosphere in the presence of β-met. (Bottom) Comparison of the emission spectra from SImaging experiments with BY-2 cells (cytoplasm with excitation at 405 or 488 nm) and the emission spectrum of **F-PDO** after irradiation at 350 nm for 2 h in the presence of β-met. [**F-PDO**] = 40 µM; [β-met] = 40 µM. Solvent: H_2O/DMSO (7:3 *v/v*) buffered at pH 6.9. λ_{exc} = 470 nm. Ox = under air atmosphere; Deox = under argon atmosphere; UV = irradiation at 350 nm for 2 h.

Other molecules of biological interest such as cysteine (Cys) and glutathione (GSH) (i.e., thiol- and amino-containing substrates, Figures S15, S16 and S18 in the ESI) have been tested with **F-PDO** in this screening assay and compared to the other investigated compounds (**F-PD**, **PD** and **PDO**). Interestingly, a very peculiar behavior has been highlighted with Cys. Incubation of **F-PDO** with Cys generated two fluorescence emission signals depending if the mixture was UV-photoirradiated or not (Figure S15 in the ESI). The presence of an intense and broad emission comparable to the one formed after β-met incubation (λ_{em} ~ 565 nm) was detected in the absence of UV-irradiation either under air or argon atmosphere. Alternatively, a markedly different broad fluorescence emission signal centered at λ_{em} ~ 545 nm was observed under irradiation at 350 nm of **F-PDO** for 2 h in the presence of air oxygen or argon (Table 1). **F-PDO** is the most oxidizing derivative (E^1_{red} = -0.33 V) likely to be chemically reduced by Cys unlike the other analogues. Interaction of **F-PDO** with Cys alone thus appears to be sufficient to generate a fluorescent species responsible for the emission at ~ 570 nm. These data thus suggest that **F-PDO** could be reduced either photochemically or by Cys and could lead to adducts with this biomolecule either by attack of thiol or amine functions. An emission of lower intensity and centered at ~ 540-550 nm was indeed evidenced with amine derivatives such as lysine (Lys) or histidine (His)

(*vide infra*). Comparison with other naphthoquinone-derived compounds also revealed a peculiar behavior of **F-PD** towards Cys upon UV-irradiation with an intense emission centered at 584 nm and an excitation spectrum with the main absorption band centered at about 494 nm. The other compounds, **PD** and **PDO** lacking fluorine substitution on the methyl group of the menadione subunit, are slightly or not reactive in the presence of Cys suggesting a markedly different behavior of **F-PD** and **F-PDO** towards Cys compared to β-met. It is important to note that Cys exists as a zwitterionic species at pH 6.9 and that the thiol function is not ionized (R-SH: pK_a = 8.91)[47] under these experimental conditions. While **F-PDO** induces an emission signal even in the absence of UV-irradiation with Cys, none of the other investigated compounds displayed an emission signal in the absence of UV-irradiation. The presence or absence of oxygen during the photochemical reaction has no effect on the observed results. For **F-PD**, the influence of the UV irradiation time in the presence of Cys was examined and showed a faster reaction with a maximum of product formed already after 30 minutes of exposure to UV (Figure S17 in the ESI). In the absence of irradiation at 350 nm, no reaction was observed between **F-PD** and Cys, demonstrating the photochemical character of the interaction, unlike for **F-PDO**. Moreover, UV-irradiation of **PD** in ^{i}PrOH under air atmosphere promoted benzyl oxidation to **PDO** suggesting that the emission observed for **F-PD** and Cys would correspond to the benzyl oxidation to **F-PDO** and formation of adducts with Cys. With glutathione GSH (Figure S13 in the ESI), no particular emission was observed and only the reactions with **F-PD** and **F-PDO** stand out with an emission centered around 550 nm, similar to the observed after UV catalyzed F-PDO reaction with Cys but much weaker than those observed in the presence of β-met (Figure S18 in the ESI).

In order to deepen further our understanding of the nature of the fluorescent adducts, we then turned our attention to two amino acids without thiol function (histidine His and lysine Lys) and applied the same approach (Figures S19 and S20 in the ESI). Whatever the conditions used, the emission signal centered at ~ 540-570 nm remains weak demonstrating the low reactivity of these amino acids towards the benz(o)yl-menadiones studied. This also seems to indicate that the amine or carboxylate functions are less involved in the reactions monitored during this screening assay. In parallel, **F-PDO** was shown to be the only benz(o)ymenadione capable of alkylating a model protein such as Bovine Serum Albumin (BSA) following irradiation at 350 nm (Figure S21 in the ESI). Table 1 summarizes the emission data obtained with **F-PDO**, **F-PD**, **PD** and **PDO** and the different substrates, and it clearly emphasizes the peculiar reactivity of **F-PDO** (and to a lesser extent **PDO** and **F-PD**) with biological-relevant thiol-containing substrates such as cysteine or with model proteins such as BSA.

Table 1. Emission data measured for **F-PDO**, **F-PD**, **PD** and **PDO** (40 µM) and various substrates (40 µM) in the screening assay. λ_{exc} = 470 or 440 nm, UV-irradiation at 350 nm (Rayonet photochemical reactor 224 W) for 2 h or for *h*GR NADPH cycling for 2 h, Argon atmosphere. Dark green: high emission intensity. Light green: moderate emission intensity. Light grey: weak emission intensity. nd: not determined. Nr: no reaction.

Compd.	**Thiol (SH)**	**Mixed (SH, NH_2)**						**Amines (NH_2)**	
	β-met (UV)	Cys (UV)	GSH (UV)	BSA (UV)	BSA (NADPH)	*h*GR (NADPH)	BSA + *h*GR (NADPH)	Lys (UV)	His (UV)
PD	560	580	555	545	nd	nd	nd	545	545
PDO	**564**	575	555	545	nd	nd	nd	545	545
F-PD	550	**583**	**560**	570	nr	522	520	570	570
F-PDO	**570**	**570** (-UV) **545** (+UV)	**545**	**555**	580	**525**	**525**	545	545

Applying the same screening strategy, the ability of **F-PDO** and **F-PD** to fluorescently probe relevant proteins such as BSA (1 free thiol Cys34[48]) or human glutathione reductase (hGR, 10 cysteines) was then evaluated. We have previously demonstrated that **PDO** is an effective subversive substrate for both NADPH-dependent *h*GR[28] and *Pf*GR.[49] **PDO**, a metabolite resulting from the bioactivation (benzylic oxidation) of **PD** prodrug, is able to enter a redox cycle with reductase enzymes under NADPH flux, generating the one- and two-electron reduced species. This enzymatic reduction, previously mimicked by UV-irradiation, thus generates a reactive *o*-QM intermediate capable, like fluoro-M5 (Scheme 1F), of alkylating thiol residues of the enzyme and thus acting as a suicide substrate. The fluorescence emission response observed in particular with *h*GR (Figure S22 in the ESI) thus clearly demonstrated the ability of **F-PDO** to label *h*GR efficiently. This is in excellent agreement with previously published data obtained with the fluoro-M5 analogue, likely by generating covalent adducts with free thiol units (Scheme 1F).[13,42]

Emission Properties under UV-irradiation. Following this study, the emission properties of **F-PDO** in the presence and absence of β-met under UV-irradiation was then studied. In the absence of photoirradiation, it has been reported that menadione can react with cysteine or glutathione (i.e., likely after reduction by the reducing biomolecules) to lead to a thioether adduct[33,50] (e.g., with GSH, the thioether adduct 2-methyl-3-glutathionyl-1,4-naphthoquinone is also termed thiodione, Figure 7) that display emission maximum at 480 nm (λ_{exc} = 340 nm) and 420 nm (λ_{exc} = 360 nm) for cysteine and glutathione, respectively.[51] In the absence of biological thiols, electrochemical or photochemical reduction of menadione also generate a fluorescent dihydronaphthoquinone species emitting at much higher energies (λ^{em} = 420 nm) upon excitation at 309 nm.[44,52]

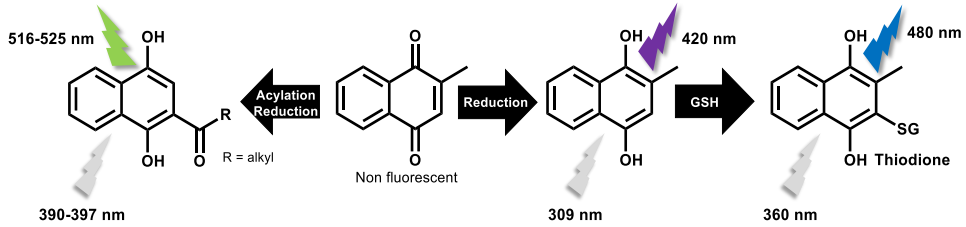

Figure 7. Chemical structures and emission properties of 1,4-naphthoquinone derivatives under their 2e-reduced form reported from literature.

From the viewpoint of organic synthesis, a visible light-induced thiolation of substituted 1,4-naphthoquinones was recently developed using various thiol derivatives and eosin as the photoredox catalyst.[53] On the other hand, a *α*-selective Csp_3–H bond functionalization of primary aliphatic alcohols with 1,4-naphthoquinones driven by blue-LED light irradiation in the absence of catalyst, metal, base or reagent afforded a large series of 2-acylated-1,4-naphthohydroquinones that were shown to display a fluorescent signal in the visible region (Figure 7).[54] For example, the maxima of absorption (λ^{abs}) and of emission (λ^{em}) were found to be 393 and 516 nm, respectively, for 2-acetyl-1,4-naphthohydroquinone in acetonitrile substantiating our preliminary findings (Figure 7).

To deepen the understanding of the fluorescence properties of **F-PDO**, experiments were performed in an ^{i}PrOH/DCE (*v/v*) mixture ([**F-PDO**] = 0.25 mM) under irradiation at 350 nm (Rayonet photochemical reactor 224 W). Whether in the presence or the absence of β-met, a UV-irradiation for 2 h 15 resulted in the formation of a new absorption band centered at ~ 435 nm and 415 nm in the absence and presence of β-met, respectively. Regardless of the presence of β-met, no spectral alteration of **F-PDO** could be observed in the absence of UV-irradiation (Figure 8) confirming that photoreduction to semi-naphthoquinone or dihydronaphthoquinone is the process at the origin of these spectral alterations in agreement with literature data (*vide supra*). In addition, comparison of

the absorption spectra of **F-PDO** in the absence and presence of β-met highlighted substantial spectral differences (Figure S23 in the ESI). Excitation at 435 nm of **F-PDO** with and without β-met gives rise to a bright structured emission of vibronic nature (~ 1400 cm^{-1}) whose maxima are centered at 530, 570 and 620 nm for both systems (Figure 8). The measurement of excitation spectra by analysis at emission maxima (530, 570 and 620 nm) clearly demonstrates that it is a single emitting species (Figure S24 in the ESI) with a sizeable Stokes shift of about 95 nm. The vibronic structure of the **F-PDO** emission and excitation is likely a signature of a restricted excited state that is more planar than in the ground state (i.e., the absorption band of the photoactivated **F-PDO** is broad with however, a less marked vibronic progression).

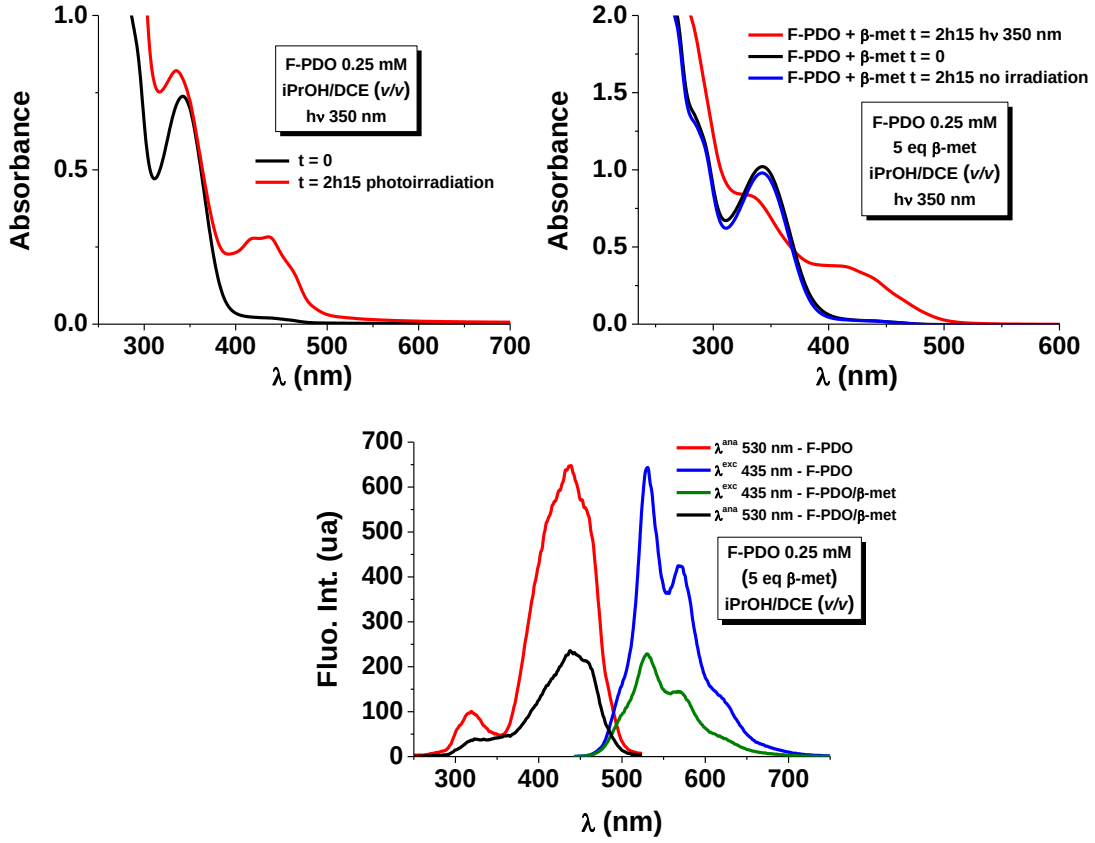

Figure 8. (Top) Absorption spectra of **F-PDO** in the absence (left) and in the presence (right) of 5 equivalents of β-met before and after irradiation at 350 nm (Rayonet photochemical reactor 224 W) for 2 h 15 in ^{i}PrOH/DCE (*v/v*). [**F-PDO**] = 0.25 mM. (Bottom) Emission (λ^{exc} = 435 nm) and excitation (λ^{ana} = 530 nm) of **F-PDO** in the absence and in the presence of 5 equivalents of β-met after irradiation at 350 nm (Rayonet photochemical reactor 224 W) for 2 h 15 in ^{i}PrOH/DCE (*v/v*). [**F-PDO**] = 0.25 mM. Excitation and emission bandwidths = 4 nm.

Comparison of the emission and excitation spectra recorded for **F-PDO** in the absence or presence of β-met under the same experimental conditions suggests a structural similarity with, however, minor differences in the emission and excitation spectra and in their brightness (Figure S25 in the ESI). This would indicate that, following photoirradiation, the adduct formed with β-met has a structure close to the photoactivated **F-PDO** species. We then turned our attention to **PDO** and performed the same series of experiments. Although the data obtained (Figures S26 and S27 in the ESI) suggest the formation of similar species, **PDO** was found to be far less responsive than **F-PDO** demonstrating clearly the less oxidizing character of **PDO** (E^{1}_{red} = -0.46 V) with respect to **F-PDO** (E^{1}_{red} = -0.33 V) as well as the importance of fluorination in the photoactivation of **F-PDO** to lead to a reactive *o*-QM species (Scheme 1). The emission properties of **PDO(2'F)**, a positional isomer of **F-PDO**, bearing a fluorine atom in the

2' position of the benzoyl subunit was next examined. As observed with **F-PDO** and **PDO**, UV-irradiation for 18 h of **PDO(2'F)** in ^{i}PrOH/DCE (*v/v*) results in the appearance of fluorescence emission centered at 540 nm. As for **PDO**, **PDO(2'F)** is much less reactive than **F-PDO** in agreement with its electrochemical properties (E^{1}_{red} = -0.45 V).[23] The emission maxima of the photoproduct are red-shifted by about 10 nm compared to those formed with **PDO** and **F-PDO** due to the presence of the fluorine atom in the 2' position of the benzoyl unit. Furthermore, upon photoirradiation, **PDO(2'F)** does not lead to a benzoxanthone derivative identified as an oxidative phenolic coupling product, the latter being characterized by a markedly different blue emission (Figure S28 in the ESI). These data are in agreement with those obtained under quasi-physiological conditions (*vide supra*). Comparison of the photophysical data of **F-PDO**/β-met mixtures recorded in ^{i}PrOH/DCE (*v/v*) (Figure 8) or in H_2O/DMSO (7:3 *v/v*) (Figure 6) suggest adducts of the same nature whose emission maximum and shape are likely influenced by the nature (polarity and proticity) of the solvent (Figure S29 in the ESI). The emission data gathered for **F-PDO**, **F-PD**, **PD** and **PDO** (λ_{em} > 540-550 nm) with β-met and Cys (and to a lesser extent with GSH) in H_2O/DMSO (7:3 *v/v*) and of **F-PDO** with β-met in ^{i}PrOH/DCE (*v/v*) are therefore markedly different from those of menadione (under reduced state, λ^{em} = 420 nm) or from thiolation of the 1,4-naphthoquinone core (under reduced state, λ^{em} = 480 nm) in position 3 (i.e., the benzyl- **(F)-PD** or benzoylMD **(F)-PDO** prevent such thiolation reaction) but are comparable to those measured for 2-acylated-1,4-naphthohydroquinones (λ_{em} 516-525 nm) thus indicating that the acyl and/or the thiol units induce a significant bathochromic shift of the emission signal of the $2e^{-}$ reduced species. To the best of our knowledge, there are no report on 1,4-naphtho(hydro)quinone compounds containing both an acetylated unit and a thioether unit at the 2,3-positions.[55] Whatever the conditions (electrochemical, chemical or photochemical conditions) described in the literature or in this study, the reduced naphthoquinone derivatives thus unambiguously corresponds to the emitting species.[52,56,57] The peculiar emission properties of **F-PDO** with or without thiols could be thus attributed to an Excited State Intramolecular Photoinduced Transfer (ESIPT) mechanism[58] (keto-enol tautomerization, Figure 9) induced by the presence of the benzoyl moiety and the formation of strong hydrogen bonding between the dihydronaphthoquinone core and the acyl residue (Figure 9). This ESIPT process can be influenced by the nature of the solvent and has been described for closely related chemical structures such as *ortho*-hydroxy-acetophenone and derivatives,[59,60] 2,5-dihydroxyacetophenone[61] or 1-hydroxy-2-acetonaphthone[62-65] to cite a few (Figure 9).

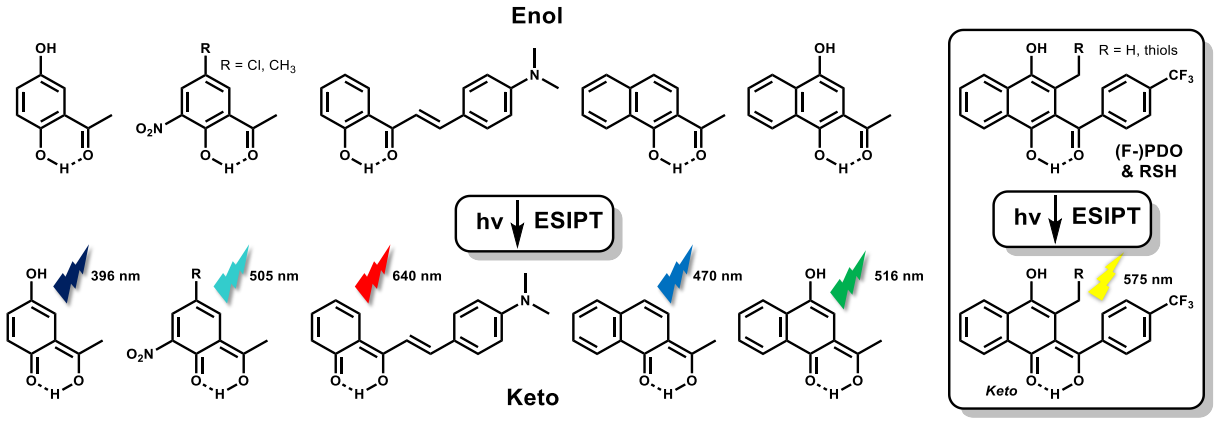

Figure 9. ESIPT properties of **F-PDO** and related compounds from literature.

Characterization of the Adducts with F-PDO under UV-irradiation Conditions. Upon photoirradiation of **F-PDO** alone for 24 h in an ^{i}PrOH/DCM (*v/v*) mixture, the formation of a homodimeric species (Figure 5A) could only be characterized and suggested. This strongly suggests that photoirradiation of **F-PDO** affords a reactive intermediate that undergoes homocoupling or Diels-Alder reaction (Scheme 5). No

radical-radical heterocoupling reactions or oligomers formation could be evidenced on the basis of the ESI-HRMS data (Figure S30 and Table S3 in the ESI) performed under these experimental conditions. Furthermore, isolation and characterization of the homodimeric species substantiate the proposed chemical structure (Figure 5B). Addition of 1 or 5 equivalents of β-met to a 5 mM solution of **F-PDO** in ^{i}PrOH/DCM (*v/v*) clearly shows the formation of a various covalent β-met adduct with **F-PDO**. Whatever the species analyzed, the ionization of the characterized species very often results from the addition of a Na^+ or K^+ cation. At the beginning of the photoirradiation, only **F-PDO** derived ions could be observed such as [**F-PDO** + Na]$^+$ (m/z_{theo} = 385.0464) or [**F-PDO** + K]$^+$ (m/z_{theo} = 401.0203). Non-covalent dimers (ion-molecule adduct) such as [(**F-PDO**)$_2$ + Na]$^+$ (m/z_{theo} = 747.1030) or ion-molecule adducts with β-met such as [**F-PDO** + β-met + Na]$^+$ (m/z_{theo} = 463.0603) or [**F-PDO** + β-met + K]$^+$ (m/z_{theo} = 479.0342) (Figure 10) were also characterized (Figures S31-S33, Table S4-S6 in the ESI). These species present at the beginning of the photoredox reaction thus vanished progressively and are switched to several covalent adducts corresponding to the loss of a fluorine atom and the incorporation of β-met subunits. A first covalent adduct **F-PDO**-β-met (Figure 10) already predominant from 7 h of reaction appears in the form of monomer ionized by Na^+ or K^+ ions, reduced species or dimeric ion-molecule under various redox states (Table 2 and Figure 10, Figures S31-S33, Table S4-S6 in the ESI). For example, characteristic peaks for [**F-PDO**-β-met + Na]$^+$ (m/z_{theo} = 443.0541), [**F-PDO**-β-met + K]$^+$ (m/z_{theo} = 459.0280) were clearly identified for the oxidized **F-PDO**-β-met covalent adduct. Ion-molecule dimeric species of the **F-PDO**-β-met species were also observed (Table 2 and Figure 10). Interestingly, **F-PDO**-β-met could undergo sequential photoredox reactions and two other covalent β-met adducts with **F-PDO** could also be evidenced. The first referred to as **F-PDO**-β-met* involves a new photoredox reaction generating a new *o*-QM followed by an intramolecular 1,4-addition of the primary alcohol function of the β-met subunit and the generation of an original 5-membered 1,3-oxathiolane ring (Scheme ***6.***). Many characteristic signals of this species can be observed from ESI-HRMS analyses such as [**F-PDO**-β-met* + Na]$^+$ (m/z_{theo} = 441.0385) or its dimeric form [(**F-PDO**-β-met*)$_2$ + Na]$^+$ (m/z_{theo} = 859.0871). From the same *o*-QM arising from **F-PDO**-β-met species, an intermolecular reaction with β-met in excess can generate a new species incorporating two β-met subunits on the same 2-methyl unit. This disulfanylation reaction is quite uncommon, favored in excess of β-met and at high concentrations, and assessed by the species [**F-PDO**-(β-met)$_2$ + Na]$^+$ (m/z_{theo} = 519.0524) and [**F-PDO**-(β-met)$_2$ + K]$^+$ (m/z_{theo} = 535.0263) and their reduced forms [**F-PDO**-(β-met)$_2$ + 2H + Na]$^+$ (m/z_{theo} = 521.0681) and [**F-PDO**-(β-met)$_2$ + 2H + K]$^+$ (m/z_{theo} = 537.0419) (Table 2 and Figure 10, Figures S31-S33, Table S4-S6 in the ESI). Therefore, sequential photoredox reactions of **F-PDO** in the presence of β-met can lead to the formation of various and original sulfanylated products that result from continuous production of reactive *o*-QM under photoirradiation capable of associating intra- or intermolecularly with thiols (i.e., β-met). A putative mechanism is proposed in Scheme 6. showing the initiation of the reaction by the formation of an *o*-QM reactive intermediate followed by sequential activation/addition or thiols together with ring closure reactions. Similar experiments were performed with **PDO** and β-met to characterize covalent adducts by ESI-HRMS (Figure S34 and Table S7 in the ESI). Only monosulfanylation of **PDO** was evidenced as compared to similar experiments carried out with **F-PDO** reinforcing the lesser reactivity of **PDO** and formation of reactive *o*-QM compared to its fluorinated congener.

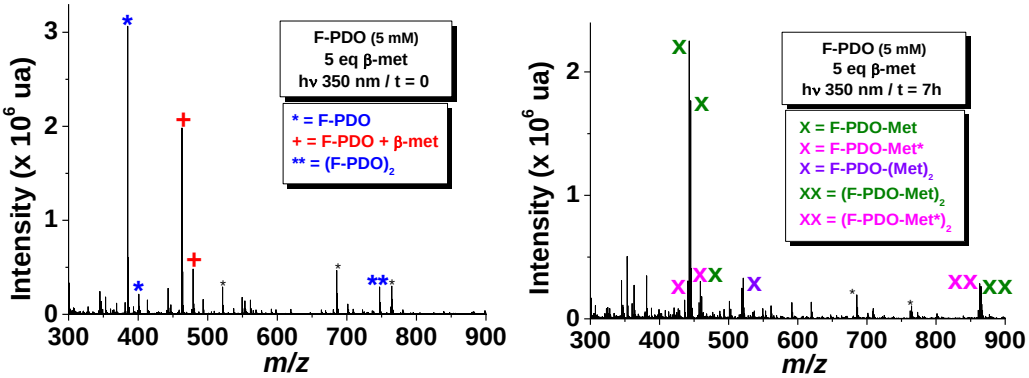

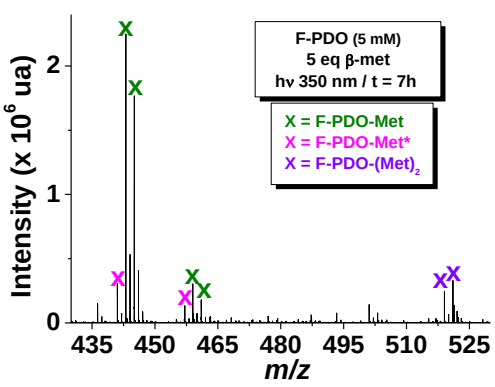

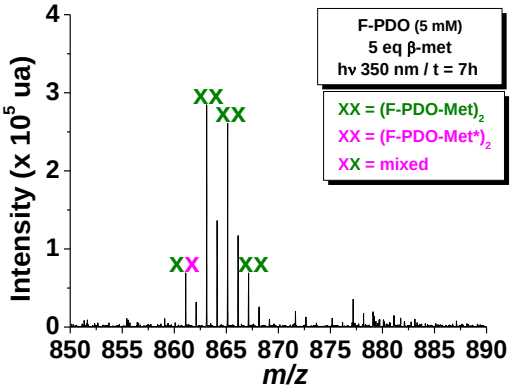

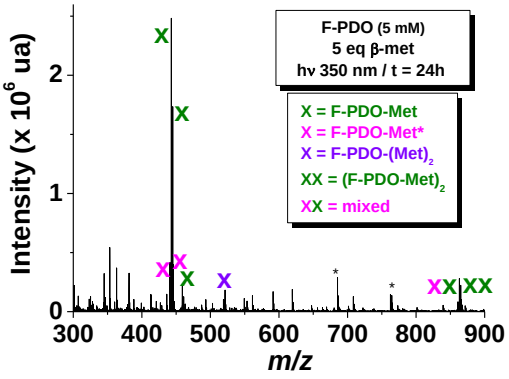

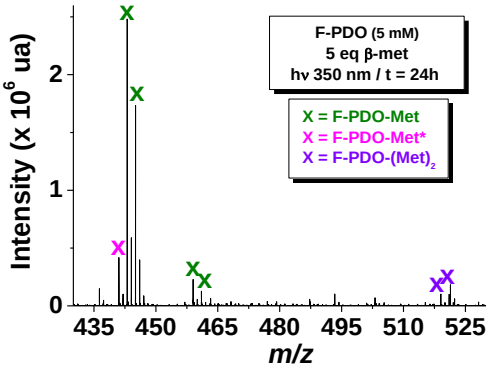

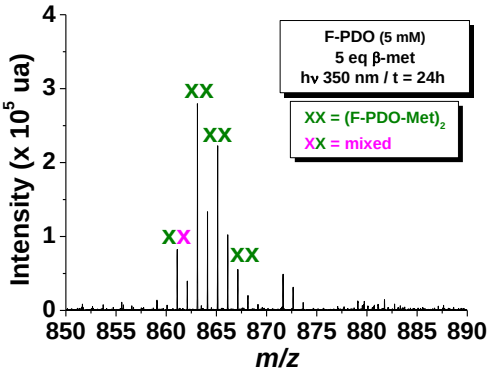

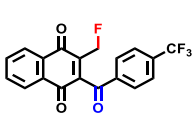

(*) F-PDO
(**) $(F\text{-}PDO)_2$

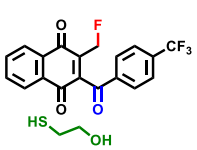

(+) F-PDO + β-met

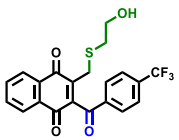

(X) F-PDO-β-met
(XX) $(F\text{-}PDO\text{-}\beta\text{-met})_2$

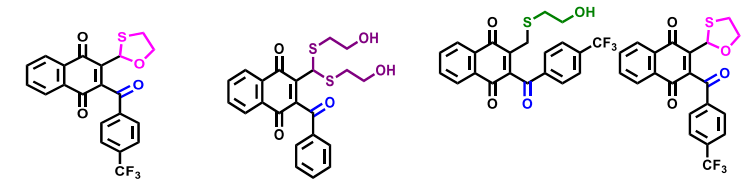

Figure 10. High Resolution electrospray mass spectra ESI-HRMS of 5 mM solution of **F-PDO** and 5 equivalents of β-met after irradiation at 350 nm (Rayonet photochemical reactor 224 W) at t = 0 and after 7 h or 24 h in ^{i}PrOH/DCM (1:1 *v*/*v*). Positive mode.

Table 2. Mono-isotopic peaks of the main species observed by ESI-HRMS (addition of Li in some cases to improve ionization of the species) for **F-PDO** (5 mM or 100 mM) and 1 or 5 equivalents of β-met irradiated at 350 nm (Rayonet photochemical reactor 224 W) for 24 h in ^{i}PrOH/DCM (*v*/*v*). The values between parentheses correspond to the differences in ppm between the experimental monoisotopic masses and the theoretical masses.

F-PDO + β-met in ^{i}PrOH/DCM – **t= 24h**				
Molecular ions	$m/z_{observed}$ 5 mM **F-PDO** 1 eq β-met	$m/z_{observed}$ 5 mM **F-PDO** 5 eq β-met	$m/z_{observed}$ 100 mM **F-PDO** 5 eq β-met	$m/z_{theoretical}$
[**F-PDO-β-met*** + Na]$^+$	441.0344 (-9.3)	441.0355 (-6.8)	441.0362 (-5.2)	441.0385
[**F-PDO-(β-met)(β-met*)** + Na]$^+$	-		517.0331 (-7.0)	517.0367
[**F-PDO-(β-met)$_2$** + Na]$^+$	-	519.0483 (-7.9)	519.0492 (-6.2)	519.0524
[**F-PDO-(β-met)$_2$** + K]$^+$	-		535.0245 (-3.4)	535.0263
[**F-PDO-(β-met)$_2$** + 2H + Na]$^+$	-	521.0656 (-4.8)	521.0638 (-8.2)	521.0681
[**F-PDO-(β-met)$_2$** + 2H + K]$^+$	-	-	537.0391 (-5.2)	537.0419
[**F-PDO-β-met** + Na]$^+$	443.0509 (-7.2)	443.0520 (-4.7)	443.0502 (-8.8)	443.0541
[**F-PDO-β-met** + K]$^+$	459.0239 (-8.9)	459.0250 (-6.5)	459.0258 (-4.8)	459.0280
[**F-PDO-β-met** + 2H + Na]$^+$	445.0669 (-6.5)	445.0680 (-4.0)	445.0662 (-8.1)	445.0698
[**F-PDO-β-met** + 2H + K]$^+$	461.0424 (-2.8)	461.0408 (-6.3)	461.0416 (-4.6)	461.0437
[**(F-PDO-β-met)$_2$** + Na]$^+$	863.1123 (-7.1)	863.1129 (-6.4)	863.1129 (-6.4)	863.1184
[**(F-PDO-β-met)$_2$** + K]+		-	879.1054 (14.9)	879.0923
[**(F-PDO-β-met)$_2$** + 2H + Na]$^+$	865.1296 (-5.2)	865.1267 (-8.6)	865.1282 (-6.8)	865.1341
[**(F-PDO-β-met)$_2$** + 2H + K]$^+$	-	-	881.1021 (-6.7)	881.1080
[**(F-PDO-β-met)$_2$** + 4H + Na]$^+$	867.1423 (-8.5)	867.1394 (-11.9)	867.1409 (-10.1)	867.1497
[**(F-PDO-β-met)$_2$** + 4H + K]$^+$	-	-	883.1190 (-5.2)	883.1236
[**(F-PDO-β-met*)(F-PDO-β-met)** + Na]$^+$	861.0973 (-5.6)	861.0979 (-4.9)	861.0979 (-4.9)	861.1021
[**(F-PDO-β-met*)$_2$** + Na]$^+$	859.0811 (-7.0)			859.0871

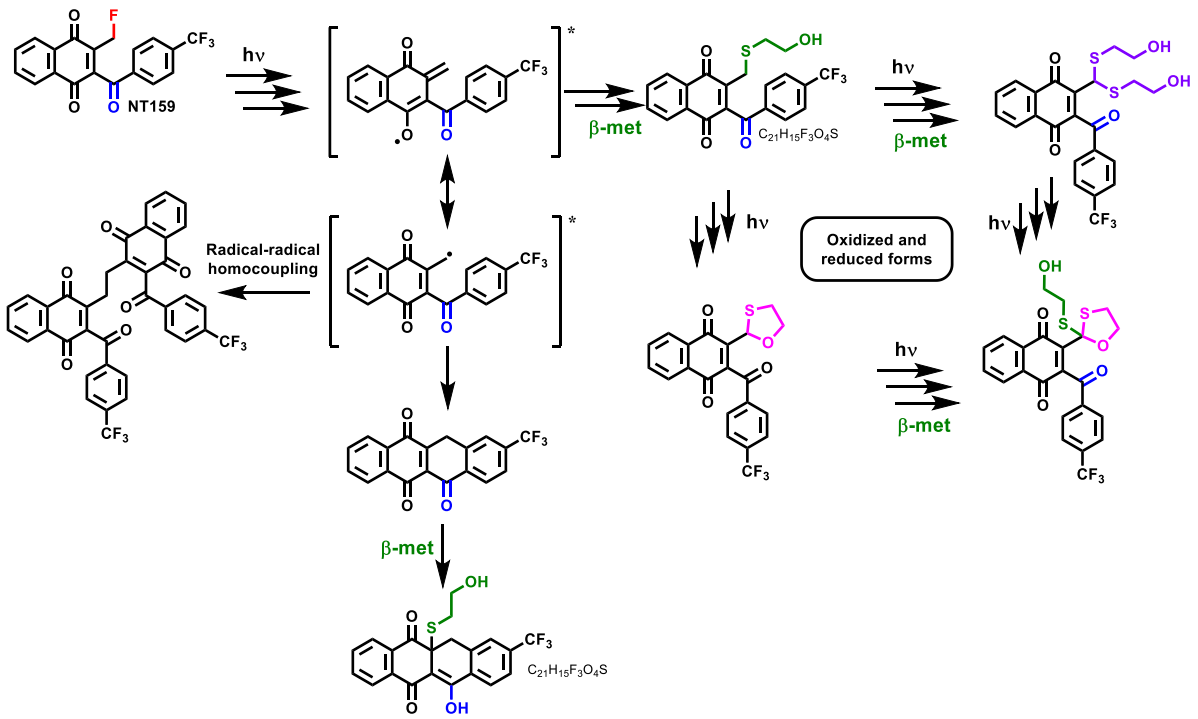

Scheme 6. Putative mechanism of sequential formation of covalent β-met adducts with **F-PDO** upon photoirradiation in ^{i}PrOH/DCM (v/v) for 24 h. Only the oxidized states are represented but the 1- and 2-e^- reduced forms have been also evidenced using ESI-HRMS detection.

Most of the products characterized in oxidized or reduced form result from the trapping of the highly reactive o-QM intermediate generated by UV-irradiation with thiol derivatives. An intramolecular coupling could also be envisaged and generate a tetracyclic anthrone-like compound potentially reactive towards thiols (Scheme 6.). Indeed, It has been shown that 2-methyl-benzophenone affords in benzene, under laser-jet conditions (i.e., high-intensity single Beam UV 334-364 nm, 2.6 W, 6 h or 2.85 W, 45 min or double crossed- UV 334-364 nm – and - visible 458-514 nm- beam) a long-lived (i.e., several seconds) photoenol-*E* intermediate that can lead to a dihydroanthrone tautomer, ultimately being oxidized to a final anthrone.[66] Irradiation with UV photons was hypothesized to favor the formation of the photoenol-*E,* while visible photons favor the conversion of the intermediate to the dihydroanthrone. Besides, it was demonstrated that photo-reversion of the dihydroanthrone to the photoenol-*E* can be favored with high-energy UV-irradiation (Figure 11). As a side product, a homodimeric species was also characterized. The same reaction performed with 2-methyl-benzophenone in benzene or ^{i}PrOH using UV irradiation (Rayonet device) did not lead to the formation of the cyclized anthrone-like species but to various dimeric products.[66] On the other hand, landomycins (benz[a]anthraquinone derivatives, Figure 11) from the angucycline family (natural antibiotics produced by *Streptomyces* bacteria) were shown, either in cell-free conditions or intracellularly, to react through the spontaneous formation of Michael adducts with biothiols (e.g., reduced cysteine or glutathione).[67] With landomycin E (LE) and *N*-acetylcycteine (NAC), the authors evidenced the formation of an oxidized LE-NAC (LE-NAC_{ox}) that can be reduced to a short-lived (several minutes) fluorescent species (LE-NAC_{red}, λ^{em} = 428 nm) that is re-oxidized to form a L-NAC_{ox} species (dissociation of the substituted sugar). LE-associated fluorescence was also observed by live-cell fluorescence microscopy in the cytoplasm and nucleus of human LN229 glioblastoma and MG63 osteosarcoma cells. These two studies thus suggest that **F-PDO** could also lead, under photoactivation, to the formation of an anthrone-like tetracyclic compound capable of associating like LE with a biothiol and allowing, according to the same mechanism, to explain the fluorescence observed both in the cytoplasm and nucleus of BY-2 tobacco cells.

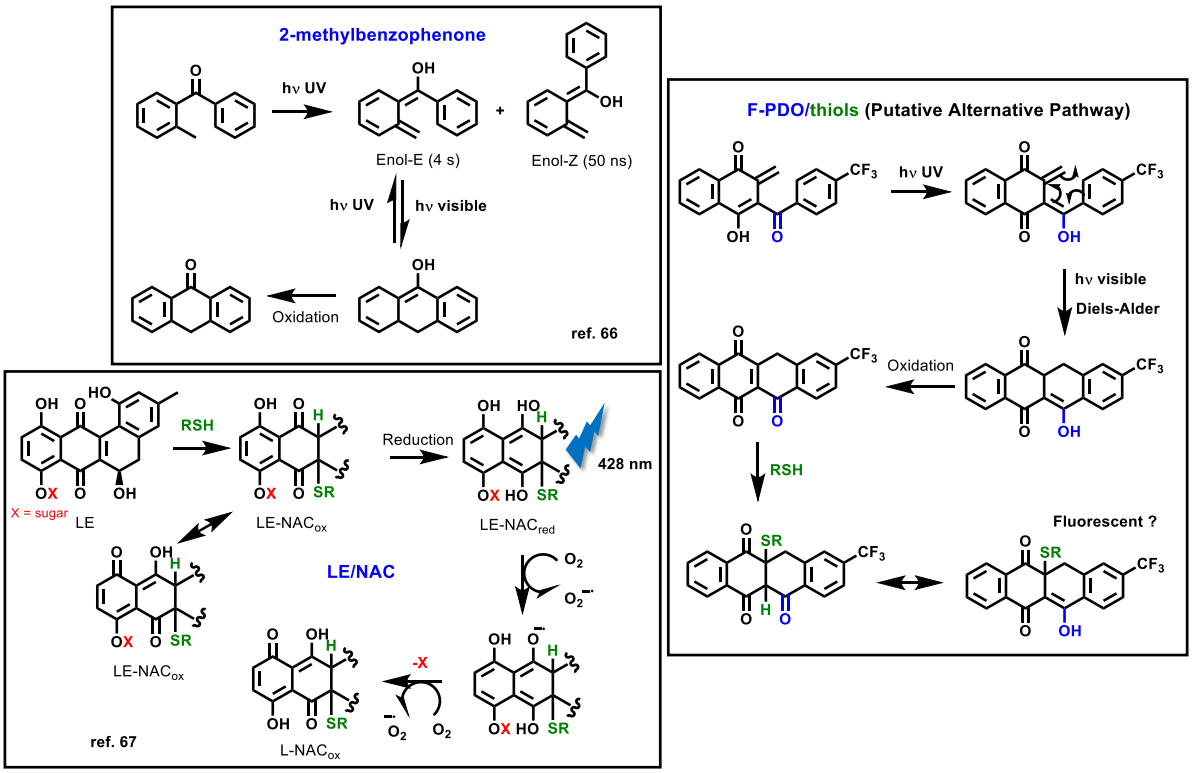

Figure 11. (Top left) Photo-assisted intramolecular cyclization to anthrone of benzophenone derivatives, (bottom left) Michael addition of thiols to landomycins and reduction-induced fluorescence, (right) putative mechanism of intramolecular photo-cyclization of **F-PDO** and subsequent addition of thiols and formation of fluorescent reduced thiol adducts with tetracyclic derivative.

In order to test the possibility of formation of anthrone-like species, **F-PDO** was first irradiated (350 nm) in benzene in the absence and presence of β-met (Figure S35 and Table S8 in the ESI). As seen previously, **F-PDO** is unreactive under these experimental conditions and mainly free or non-covalent adducts of **F-PDO** with β-met observed. Modification of the experimental conditions ([**F-PDO**] = 100 mM and 5 equivalents of β-met) and of the irradiation source (double crossed LED beams: UV 365 nm and visible 430 nm excitation with a typical output of 200 mW.cm^{-2}) allowed to substantially improve the reactivity of **F-PDO** in benzene. Most of the covalent adducts observed in ^{i}PrOH/DCM (e.g., mono and disulfanylated adducts, Figure 10) were also characterized using double crossed photoirradiation in benzene (Figure S36 and Table S9 in the ESI). In ^{i}PrOH/DCM (*v/v*), the same photoproducts were also observed using double crossed excitation beams (Figure S37 and Table S10 in the ESI). In addition, measurement of the reaction products after 24 h in daylight or in the dark in ^{i}PrOH/DCM (*v/v*) does not reveal the formation of other derivatives such as anthrones potentially related to slower reactions. At this stage, the HRMS data obtained under these new conditions do not allow however to conclude definitively bout the formation of tetracyclic species. Indeed, the β-met adduct with the anthrone-like species resulting from the photoactivation of **F-PDO** has exactly the same molecular formula as the product resulting from the monosulfanylation of **F-PDO** (Figure 10 and Table 2). To deepen our understanding of the reactivity of **F-PDO**, the anthrone analogues potentially derived from **F-PDO** in a seven-step sequence (Scheme 4) were synthesized. Surprisingly, the expected naphthacetriones were not observed due to enone-dienol tautomerism giving 6-hydroxy-8-(trifluoromethyl)tetracene-5,12-dione (**AnthraQ-PDO isomer 12a**) and 6-hydroxy-9-(trifluoromethyl)tetracene-5,12-dione **12b** (**AnthraQ-PDO**) whose driving force is most likely aromatization and intramolecular hydrogen bond formation. **AnthraQ-PDO isomers 12a-b** were fully characterized (see ESI) and their ESI-HRMS spectra recorded both in positive and negative mode (Figure S38 and Table S11 in the ESI). Due to the presence

of a phenol unit, **AnthraQ-PDO 12a-b** are more readily detectable in negative mode as evidenced by the peaks observed at *m/z* = 341.0445 ([**AnthraQ-PDO** - H]$^-$) and *m/z* = 688.0990 ([(**AnthraQ-PDO** – H)$_2$ + Li]$^-$). Negative mode HRMS analysis of a **F-PDO** solution in ^{i}PrOH/DCM (*v/v*) after 18 h of UV-irradiation does not show anthraquinone formation (Figure S38 in the ESI). Interestingly, the measurement of the spectroscopic properties of **AnthraQ-PDO 12a-b** revealed an absorption band centered at ~435 nm as well as an emission profile (Φ^{abs} = 16% for **AnthraQ-PDO 12a** and Φ^{abs} = 27% for **AnthraQ-PDO 12b** in ethanol) comparable to that of **F-PDO** without substrate after UV-irradiation at 350 nm (Figures S39 and S40 in the ESI). This suggests that the facilitated photoreduction induced by the presence of the fluorine atom within **F-PDO** generates a reduced species whose excitation leads to an ESIPT process responsible for the emission in the visible in close agreement with the data obtained for the closely related compound **AnthraQ-PDO 12a-b**.

Conclusion

In this work, the (photo-)reactivity of **F-PDO**, a plasmodione **PDO** analogue, was investigated. The introduction of a fluorine atom on the 2-methyl group drastically alters the redox properties of the 1,4-naphthoquinone electrophore making **F-PDO** highly oxidizing with respect to **PDO**. This increased reactivity makes **F-PDO** very photoreactive as well. In the absence of any nucleophile, photoreduction in an ^{i}PrOH/DCM mixture leads to the formation of a highly reactive *ortho*-quinone methide capable of generating a homodimer that was synthesized and fully characterized. In the presence of nucleophiles such as thiols of which β-mercaptoethanol was used as a model in this study, several adducts were characterized, most of them constituting very original chemical structures. Indeed, under photoreduction, the *o*-QM is continuously regenerated and this sequential photoredox reactions could afford mono- or disulfanylation products that were characterized by ESI-HRMS. The selectivity of **F-PDO** over related analogues such as **F-PD**, **PD** or **PDO** toward relevant nucleophiles (β-mercaptoethanol, cysteine, GSH, Histidine, Lysine or BSA) using plate-reading in the fluorescence emission mode allowed us to highlight the peculiar properties of **F-PDO** with respect to thiol containing nucleophiles. **F-PDO** is therefore a relevant derivative capable of alkylating proteins (e.g. BSA used in this study) upon photo- or enzymatic reduction, as shown upon activation by *h*GR under NADPH flux. Noteworthy, the reduced species derived from **(F)-PDO** exhibit emission properties in the visible region, making them valuable fluorescent probes for monitoring protein alkylation processes, but also for monitoring the redox status within living cells such as BY-2 tobacco cells. These emission properties are closely related to the ability of benzoyl-menadiones to generate under (photo)-reduction reduced species capable of leading to ESIPT process. Thus, a very large Stokes gap of about 95 nm and a characteristic bright yellowish emission are achieved. The fluorescence response is enhanced in the case of **F-PDO** due to its high reactivity and its propensity to be reduced more easily. Upon photochemical activation of **F-PDO**, the generated *o*-QM is likely to react to lead to the intramolecular formation of an anthrone, which can also explain the fluorescence emission observed in BY-2 cells. Although never identified in high resolution mass spectrometry studies, a methodology to access these anthrone-like derivatives was developed. Interestingly, tautomerization occurs and the most stable products were demonstrated to be hydroxy-anthraquinones (**AnthraQ-PDO**, Figure 2**)**. These compounds, in their oxidized form, exhibit emission properties comparable to those of reduced **F-PDO** species, which can be rationalized in view of their comparable chemical structure to those resulting from ESIPT processes. In conclusion, a subtle modification of **PDO** allowed access to **F-PDO** that constitutes a promising (pro)-fluorescent chemical tool to follow the activation (i.e. reduction) and alkylation of proteins in living cells by cell imaging thus paving the way for the development of innovative molecular tools for the monitoring and labeling of target proteins.

Experimental section.

General Information.

Compounds **PD**, **PDO** and **PD-bzol** were synthesized according to reported procedures.[23,26,49]. Starting materials, reagents and dry solvents were obtained from Sigma-Aldrich, ABCR GmbH & Co., Alfa Aesar, Fluorochem and Apollo Scientific and used without further purification. Solvents were obtained from Carlo Erba, VWR and Fisher Scientific. All reactions were performed in standard glassware. Thin-layer chromatography (TLC) were performed using Merck silica gel plates (60 F-254, 0.25 mm) on aluminum sheets and revealed under UV lamp (325 and 254 nm). Crude mixtures were purified by flash column chromatography on silica gel 60 (230-400 mesh, 0.040-0.063 mm) purchased from VWR. NMR spectra were recorded on a Bruker Avance 400 apparatus (^{1}H NMR, 400 MHz - ^{13}C NMR, 101 MHz - ^{19}F NMR, 377 MHz) or Bruker Avance III HD 500 MHz apparatus (^{1}H NMR, 500 MHz - ^{13}C NMR, 126 MHz - ^{19}F NMR, 471 MHz) at the ECPM. All chemical shifts (δ) are quoted in parts per million (ppm). The chemical shifts are referred to the used partial deuterated NMR solvent ($CDCl_3$: ^{1}H NMR, 7.26 ppm and ^{13}C NMR, 77.16 ppm). The coupling constants (J) are given in Hertz (Hz). Resonance patterns are reported with the following notations: s (singlet), d (doublet), t (triplet), q (quartet), m (multiplet), tt (triplet of triplets). High-resolution mass spectrometry (HRMS) analyses were performed with a Bruker MicroTOF mass analyzer under ESI in the positive mode detection (measurement accuracy ≤15 ppm) at the Service de Spectrométrie de Masse Fédération Chimie Le Bel in Strasbourg.

2-(fluoromethyl)-3-(4-(trifluoromethyl)benzyl)naphthalene-1,4-dione, F-PD (3). To a solution of 2-(fluoromethyl)-1,4-dihydronaphthalene-1,4-dione **2** (0.69 g, 3.6 mmol, 1.0 equiv.) and 4-(trifluoromethyl)phenylacetic acid (1.1 g, 5.4 mmol, 1.5 equiv.) in a mixture of MeCN (56 mL) and H_2O (19 mL), was added $AgNO_3$ (0.22 g, 1.3 mmol, 0.35 equiv.) followed by $(NH_4)_2S_2O_8$ (1.1 g, 4.7 mmol, 1.3 equiv.). The mixture was then stirred at reflux (DrySyn heating block) for 3 h and protected from light. After this time, the aqueous layer was extracted three times with DCM. The combined organic layers were washed with a saturated aqueous solution of $NaHCO_3$, dried over $MgSO_4$ and concentrated under reduced pressure. The crude mixture was purified by flash chromatography on silica gel using toluene 100% as eluent to afford **3** as a yellow solid (0.46 g, 37%). **mp** 78°C. **^{1}H NMR (500 MHz, $CDCl_3$):** *δ* 8.14-8.09 (m, 1H), 8.09-8.04 (m, 1H), 7.78-7.69 (m, 2H), 7.56-7.50 (m, 2H), 7.44-7.38 (m, 2H), 5.59 (d, *J* = 47.0 Hz, 2H), 4.20 (s, 2H). **^{13}C {H} NMR (126 MHz, $CDCl_3$):** *δ* 184.7, 183.7 (d, $^{3}J_{C\text{-}F}$ = 2.5 Hz), 148.5 (d, $^{3}J_{C\text{-}F}$ = 4.0 Hz), 141.6, 139.4 (d, $^{2}J_{C\text{-}F}$ = 11.7 Hz), 134.4, 134.2, 131.9, 131.7, 129.4, 129.3, 129.1 (q, $^{2}J_{C\text{-}F}$ = 32.3 Hz), 126.9, 126.7, 125.7 (q, $^{3}J_{C\text{-}F}$ = 3.8 Hz, 2C), 124.2 (q, $^{1}J_{C\text{-}F}$ = 271.8 Hz), 75.9 (d, $^{1}J_{C\text{-}F}$ = 167.0 Hz), 32.3. **^{19}F NMR (377 MHz, $CDCl_3$):** *δ* -62.54 (3F), -217.84 (tt, *J* = 46.9, 2.4 Hz). **HRMS (ESI+)** *m/z*: $[M+H]^+$ calculated for $C_{19}H_{13}F_4O_2$: 349.0846, found 349.0835.

(3-(fluoromethyl)-1,4-dimethoxynaphthalen-2-yl)(4-(trifluoromethyl)phenyl)methanone (4). In a flame-dried flask, under argon, to a solution of 2-bromo-3-(fluoromethyl)-1,4-dimethoxynaphthalene **1** (1.7 g, 5.5 mmol, 1.0 equiv.) in dry THF (11 mL) was added dropwise *n*-BuLi (1.6 M in hexane, 4.0 mL, 6.3 mmol, 1.2 equiv.) at -78 °C. The reaction mixture was then stirred for 10 min at -78 °C. 4-(trifluoromethyl)benzoyl chloride (1.2 mL, 7.8 mmol, 1.4 equiv.) was added in one portion, and allowed to react for 50 min at -78 °C under vigorous stirring. After this time, the reaction mixture was allowed to return to room temperature and a 3 M HCl aqueous solution was then added to the resulting mixture. The aqueous layer was extracted three times with Et_2O. The combined organic layers were washed with brine, dried over $MgSO_4$ and evaporated under reduced pressure. The crude residue was purified by flash chromatography on silica gel (Toluene/Cyclohexane 4:1) giving **4** as a yellow-green oil (1.8 g, 83% yield). **mp** 98°C. **^{1}H NMR (500 MHz, $CDCl_3$):** *δ* 8.25-8.20 (m, 1H), 8.15-8.09 (m, 1H), 8.02-7.96 (m, 2H), 7.74-7.70 (m, 2H), 7.69-7.63 (m, 2H), 5.59 (d, *J* = 47.6 Hz, 2H), 4.03 (s, 3H), 3.78 (s, 3H). **^{13}C {H} NMR (126 MHz, $CDCl_3$):** *δ* 195.9, 152.6 (d, $^{3}J_{C\text{-}F}$ = 6.3 Hz), 150.3 (d, $^{4}J_{C\text{-}F}$ = 2.3 Hz), 140.5, 134.8 (q, $^{2}J_{C\text{-}F}$ = 32.6 Hz), 130.0 (2C), 129.7 (d, $^{4}J_{C\text{-}F}$ = 2.4 Hz), 129.3 (d, $^{3}J_{C\text{-}F}$ = 2.6 Hz), 129.1-128.9 (m),

128.1 (2C), 125.8 (q, $^{3}J_{C\text{-}F}$ = 3.8 Hz, 2C), 123.8 (q, $^{1}J_{C\text{-}F}$ = 272.9 Hz) 123.5, 123.0, 122.4 (d, $^{2}J_{C\text{-}F}$ = 15.7 Hz), 76.8 (d, $^{1}J_{C\text{-}F}$ = 163.8 Hz, peak hidden by chloroform signal, determined by DEPT135) , 64.3 (d, $^{5}J_{C\text{-}F}$ = 2.3 Hz), 63.7. **^{19}F NMR (471 MHz, $CDCl_3$):** δ -63.09 (3F), -203.78 (t, *J* = 47.6 Hz). **HRMS (ESI+)** *m/z*: $[M+Na]^+$ calculated for $C_{21}H_{16}F_4NaO_3$: 415.09278, found 415.0925.

2-(fluoromethyl)-3-(4-(trifluoromethyl)benzoyl)naphthalene-1,4-dione, F-PDO (5). A solution of cerium (IV) ammonium nitrate (4.4 g, 8.0 mmol, 2.1 equiv.) in H_2O (7.7 mL) was added to a solution of [3-(fluoromethyl)-1,4-dimethoxynaphthalen-2-yl][4-(trifluoromethyl)phenyl]methanone **9** (1.5 g, 3.8 mmol, 1.0 equiv.) in MeCN (11.5 mL). The mixture was then stirred at room temperature for 1 h. After this time, the aqueous phase was extracted three times with DCM and the combined organic layers were washed with brine, dried over $MgSO_4$ and evaporated under reduced pressure. The crude residue was purified by flash chromatography on silica gel using toluene 100% as eluent giving a yellow solid (1.0 g, 74% yield). **mp** 122°C. **^{1}H NMR (500 MHz, $CDCl_3$):** δ 8.17-8.12 (m, 1H), 8.09-8.04 (m, 1H), 8.02-7.97 (m, 2H), 7.87-7.78 (m, 2H), 7.77-7.71 (m, 2H), 5.52 (d, *J* = 46.3 Hz, 2H). **^{13}C {H} NMR (126 MHz, $CDCl_3$):** δ 191.9, 183.54 (d, $^{3}J_{C\text{-}F}$ = 5.4 Hz), 183.47, 143.0 (d, $^{3}J_{C\text{-}F}$ = 2.6 Hz), 141.2 (d, $^{2}J_{C\text{-}F}$ = 14.6 Hz), 138.8, 135.3 (q, $^{2}J_{C\text{-}F}$ = 32.8 Hz), 134.94, 134.91, 131.5, 131.3, 129.3 (2C), 126.9, 126.8, 126.1 (q, $^{3}J_{C\text{-}F}$ = 3.8 Hz, 2C), 123.6 (q, $^{1}J_{C\text{-}F}$ = 272.9 Hz), 78.4 (d, $^{1}J_{C\text{-}F}$ = 173.0 Hz). **^{19}F NMR (471 MHz, $CDCl_3$):** δ -63.21 (3F), -223.16 (t, *J* = 46.4 Hz). **HRMS (ESI+)** *m/z*: $[M+Na]^+$ calculated for $C_{19}H_{10}F_4NaO_3$: 385.0458, found 385.0436.

Methyl 1,4-dimethoxy-3-(4-(trifluoromethyl)benzyl)-2-naphthoate (8a). In a flame-dried flask, under argon atmosphere, was added 2-bromo-1,4-dimethoxy-3-(4-(trifluoromethyl)benzyl) naphthalene **7a** (0.54 g, 1.3 mmol, 1.0 equiv.) in dry THF (2.6 mL). The solution was cooled at -78 °C and *n*-BuLi (1.6 M in hexane, 0.92 mL, 1.5 mmol, 1.2 equiv.) was added dropwise to the solution. The reaction mixture was stirred for 5 min at -78 °C. Methyl chloroformate (0.2 mL, 2.6 mmol, 2.0 equiv.) was then added in one portion, and allowed to react for 1 hour at -78 °C. After this time, the reaction mixture was allowed to return to room temperature and a 1 M HCl aqueous solution was added to the resulting mixture. The aqueous layer was extracted three times with DCM. The combined organic layers were washed, dried over $MgSO_4$ and evaporated under reduced pressure. The crude residue was purified by flash chromatography on silica gel (DCM/*n*-Pentane, 65:35) giving **8a** as a white solid (219 mg, 42% yield). **mp** 97°C. **^{1}H NMR (400 MHz, $CDCl_3$):** δ 8.17-8.08 (m, 2H), 7.65-7.53 (m, 2H), 7.53-7.47 (m, 2H), 7.33-7.26 (m, 2H), 4.29 (s, 2H), 3.98 (s, 3H), 3.85 (s, 3H), 3.71 (s, 3H). **^{13}C{H}NMR (101 MHz, $CDCl_3$):** δ 168.1, 150.9, 150.6, 144.4, 129.5, 129.0 (2C), 128.4 (q, $^{2}J_{C\text{-}F}$ = 32.3 Hz) 128.0, 127.6, 126.6, 125.4, 125.10 (q, $^{3}J_{C\text{-}F}$ = 3.8 Hz, 2C), 125.06, 124.3 (q, $^{1}J_{C\text{-}F}$ = 271.9 Hz), 123.2, 122.7, 63.5, 62.4, 52.2, 32.9. **^{19}F NMR (377 MHz, $CDCl_3$):** δ -62.36 (3F). **HRMS (ESI+)** *m/z*: $[M+K]^+$ calculated for $C_{22}H_{19}F_3KO_4$: 443.0867, found 443.0864.

Methyl 1,4-dimethoxy-3-(3-(trifluoromethyl)benzyl)-2-naphthoate (8b). To a stirred solution of 2-bromo-1,4-dimethoxy-3-{[3-(trifluoromethyl)phenyl]methyl} naphthalene **7b** (0.35 g, 0.82 mmol, 1.0 equiv.) in dry THF (10 mL) at -78 °C was added *n*-BuLi (1.6M in hexane, 0.65 mL, 1.0 mmol, 1.2 equiv.) dropwise and the mixture was stirred 5 min at -78 °C. Methyl chloroformate (0.13 mL, 1.7 mmol, 2.0 equiv.) was added in one portion and the reaction was stirred 1 h at -78 °C (CCM, SiO_2, Toluene 100%). After returning to room temperature, the reaction mixture was quenched with 1M HCl aqueous solution and the organic phase was separated. The aqueous phase was further extracted with DCM (3 x 10 mL). The combined organic phases were washed with water (3 x 10 mL) and brine (3 x 10 mL) then dried over $MgSO_4$, filtered, and evaporated under reduced pressure. Chromatography on silica gel with toluene 100% afforded the title compound **8b** as a brown solid (217 mg, 65% yield). **mp** 74°C. **^{1}H NMR (400 MHz, $CDCl_3$):** δ 8.14-8.10 (m, 2H), 7.63-7.54 (m, 2H), 7.47 (m, 1H), 7.44-7.41 (m, 1H), 7.36-7.31 (m, 2H), 4.28 (s, 2H), 3.97 (s, 3H), 3.85 (s, 3H), 3.69 (s, 3H).). **^{13}C {H} NMR (101 MHz, $CDCl_3$):** δ 168.3,

150.9, 150.7, 141.3, 132.4, 130.6 (d, $^{2}J_{C,F}$ = 32.0 Hz), 129.6, 128.8, 128.6, 128.1, 127.7, 126.7, 125.7, 125.6 (q, $^{3}J_{C,F}$ = 3.9 Hz), 125.2, 124.3 (d, $^{1}J_{C,F}$ = 272.3 Hz), 123.3, 123.1 (q, $^{3}J_{C,F}$ = 3.9 Hz), 122.9, 63.7, 62.5, 52.3, 32.8. **^{19}F NMR (377 MHz, $CDCl_3$):** δ -62.53. **HRMS (ESI+)** *m/z*: $[M+K]^+$ calculated for $C_{22}H_{19}F_3KO_4$: 443.0867, found 443.0845.

1,4-dimethoxy-3-(4-(trifluoromethyl)benzyl)-2-naphthoic acid (9a). To a solution of methyl 1,4-dimethoxy-3-(4-(trifluoromethyl)benzyl)-2-naphthoate **8a** (0.17 g, 0.41 mmol, 1.0 equiv.) in a mixture of EtOH (0.74 mL) and H_2O (0.12 mL) was added KOH (70 mg, 1.2 mmol, 3.0 equiv.). The mixture was then heated at reflux (DrySyn heating block) for 16 h. The reaction mixture was allowed to return to room temperature. After addition of a 3 M HCl aqueous solution, the aqueous layer was extracted with dichloromethane. The combined organic layers were dried over $MgSO_4$ and evaporated under reduced pressure. The crude residue was purified by flash chromatography on silica gel (DCM/MeOH, gradient from 1:0 to 9:1) giving **9a** as a beige solid (152 mg, 94% yield). **mp** 144°C. **^{1}H NMR (400 MHz, $CDCl_3$):** δ 8.14-8.06 (m, 2H), 7.64-7.53 (m, 2H), 7.45-7.38 (m, 2H), 7.32-7.26 (m, 2H), 4.31 (s, 2H), 3.96 (s, 3H), 3.78 (s, 3H). **^{13}C {H} NMR (101 MHz, $CDCl_3$):** δ 172.5, 151.3, 151.0, 144.7, 129.9, 129.1 (2C), 128.4 (q, $^{2}J_{C-F}$ = 32.2 Hz), 128.0, 127.9, 126.9, 125.8, 125.2 (q, $^{3}J_{C-F}$ = 3.6 Hz, 2C), 124.4 (q, $^{1}J_{C-F}$ = 271.7 Hz) 123.3, 122.9 (2C), 64.0, 62.3, 33.0. **^{19}F NMR (471 MHz, $CDCl_3$):** δ -62.28. **HRMS (ESI+)** *m/z*: $[M+K]^+$ calculated for $C_{21}H_{17}F_3KO_4$: 429.0711, found 429.0695.

1,4-dimethoxy-3-(3-(trifluoromethyl)benzyl)-2-naphthoic acid (9b). To a stirred solution of methyl 1,4-dimethoxy-3-(3-(trifluoromethyl)benzyl)-2-naphthoate **8b** (0.80 g, 2.0 mmol, 1.0 equiv.) in a mixture of EtOH (23 mL) and H_2O (4 mL) was added KOH (0.34 g, 6.1 mmol, 3.0 equiv.) and the reaction was stirred 18 h at 78 °C (DrySyn heating block). After cooling down to room temperature, the reaction mixture was quenched with 3M HCl solution, diluted with water and the resulting solution was extracted with DCM (10 mL). The organic phase was separated and the aqueous phase was further extracted with DCM (3 x 10 mL). The combined organic phases were washed with water (3 x 10 mL) and brine (3 x 10 mL) then dried over $MgSO_4$, filtered, and evaporated under reduced pressure. Chromatography on silica gel with MeOH (10%) in DCM afforded the title compound **9b** as a yellow solid (750 mg, 97% yield). **mp** 128°C. **^{1}H NMR (400 MHz, $CDCl_3$):** δ 8.17-8.11 (m, 2H), 7.66-7.57 (m, 2H), 7.49 (m, 1H), 7.42-7.37 (m, 2H), 7.34-7.30 (m, 1H), 4.39 (s, 2H), 4.04 (s, 3H), 3.83 (s, 3H). **^{13}C {H} NMR (101 MHz, $CDCl_3$):** δ 171.0, 151.5, 151.4, 141.5, 132.2 (2*C)*, 130.7 (d, $^{2}J_{C,F}$ = 32.0 Hz), 130.1, 128.8, 128.2, 128.0, 127.0, 126.0, 125.6 (q, $^{3}J_{C,F}$ = 3.7 Hz), 124.4 (d, $^{1}J_{C,F}$ = 271.2 Hz), 123.6, 123.5, 123.1 (q, $^{3}J_{C,F}$ = 3.7 Hz), 123.0, 64.1, 62.5, 32.9. **^{19}F NMR (471 MHz, $CDCl_3$):** δ -62.51. **HRMS (ESI+)** *m/z*: $[M+K]^+$ calculated for $C_{21}H_{17}F_3KO_4$: 429.0711, found 429.0720.

6,11-dimethoxy-3-(trifluoromethyl)tetracen-5(12H)-one (10a). A solution of 1,4-dimethoxy-3-(4-(trifluoromethyl)benzyl)-2-naphthoic acid **9a** (0.15 g, 0.39 mmol, 1.0 equiv.) in DCM (2.9 mL) was cooled at 0 °C. TFAA (0.11 mL, 0.78 mmol, 2.0 equiv.) was then added and the reaction mixture was stirred for 10 min. After this time, TfOH (20 µL, 0.19 mmol, 0.50 equiv.) was cautiously added at 0 °C. The reaction mixture was stirred for 16 h and allowed to return to room temperature. After addition of a saturated aqueous solution of $NaHCO_3$, the aqueous layer was extracted with DCM, the combined organic layers were dried over $MgSO_4$ and evaporated under reduced pressure. The crude residue was purified by flash chromatography on silica gel DCM/*n*-Pentane 4:1) to afford **10a** as an orange solid (87 mg, 60% yield). **mp** 128°C. **^{1}H NMR (400 MHz, $CDCl_3$):** δ 8.59-8.54 (m, 1H), 8.42-8.36 (m, 1H), 8.13-8.07 (m, 1H), 7.81-7.76 (m, 1H), 7.72-7.64 (m, 1H), 7.63-7.53 (m, 2H), 4.48 (s, 2H), 4.11 (s, 3H), 4.01 (s, 3H). **^{13}C {H} NMR (101 MHz, $CDCl_3$):** δ 183.3, 156.2, 148.8, 142.6, 134.1, 131.0, 129.7 (q, $^{2}J_{C-F}$ = 33.0 Hz), 129.4, 129.2, 128.9, 128.7 (q, $^{3}J_{C-F}$ = 3.4 Hz) 126.6, 126.3, 124.95 (q, $^{3}J_{C-F}$ = 4.0 Hz), 124.93, 124.0 (q, $^{1}J_{C-F}$ = 272.3 Hz), 121.9, 120.9, 63.4, 61.3, 27.6. **^{19}F NMR (377 MHz, $CDCl_3$):** δ -62.58. **HRMS (ESI+)** *m/z*: $[M+K]^+$ calculated for $C_{21}H_{15}F_3KO_3$: 411.0605, found 411.0592.

6,11-dimethoxy-2-(trifluoromethyl)tetracen-5(12H)-one (10b). To a stirred solution of 1,4-dimethoxy-3-(3-(trifluoromethyl)benzyl)-2-naphthoic acid **9b** (0.43 mg, 1.1 mmol, 1.0 equiv.) in DCM (8 mL) at 0 °C under argon atmosphere was added TFAA (0.32 mL, 2.3 mmol, 2.1 equiv.). After 10 minutes, TfOH (48 µL, 0.54 mmol, 0.49 equiv.) was added cautiously, the reaction mixture was allowed to warm up slowly to room temperature and stirred 16 h (CCM, SiO_2, DCM/*n*-Pentane 1:1). The reaction mixture was quenched with saturated aqueous solution of $NaHCO_3$ (2 x 10 mL) and the organic phase was separated. The aqueous phase was further extracted with DCM (3 x 10 mL). The combined organic phases were washed with water (3 x 10 mL) and brine (3 x 10 mL) then dried over $MgSO_4$, filtered, and evaporated under reduced pressure. Chromatography on silica gel with DCM/*n*-Pentane 1:1 afforded the title compound **10b** as a brown solid (240 mg, 59%). **mp** 192°C. **^{1}H NMR (400 MHz, $CDCl_3$):** δ 8.43-8.39 (m, 2H), 8.14-8.12 (m, 1H), 7.79 (m, 1H), 7.72-7.68 (m, 2H), 7.62-7.58 (m, 1H), 4.51 (s, 2H), 4.13 (s, 3H), 4.02 (s, 3H). **^{13}C {H} NMR (101 MHz, $CDCl_3$):** δ 183.7, 156.2, 148.8, 139.6, 136.5, 134.0 (d, $^2J_{C,F}$ = 32.6 Hz), 131.1, 129.5, 128.9, 128.4, 126.7, 126.5, 125.6 (q, $^3J_{C,F}$ = 3.7 Hz), 125.0, 124.0 (d, $^1J_{C,F}$ = 272.9 Hz), 123.9 (q, $^3J_{C,F}$ = 3.6 Hz), 122.0, 121.2, 63.5, 61.4, 27.7. **^{19}F NMR (377 MHz, $CDCl_3$):** δ -63.00. **HRMS (ESI+)** *m/z*: $[M+K]^+$ calculated for $C_{21}H_{15}F_3KO_3$: 411.0605, found 411.0614.

6-hydroxy-8-(trifluoromethyl)tetracene-5,12-dione (12a). In a flame-dried flask, under an argon atmosphere, were added 6,11-dimethoxy-3-(trifluoromethyl)tetracen-5(12H)-one **10a** (23 mg, 0.062 mmol, 1.0 equiv.) and TBAI (46 mg, 0.12 mmol, 2.0 equiv.) in dry DCM (1.2 mL). The mixture was cooled at -78 °C and BCl_3 (1.0 M in heptane, 0.19 mL, 0.19 mmol, 3.0 equiv.) was added. The reaction mixture was stirred for 16 h and allowed to return to room temperature. After this time, a saturated aqueous solution of Na_2CO_3 was added and the aqueous layer was extracted with DCM. The combined organic layers were dried over $MgSO_4$ and evaporated under reduced pressure. The crude residue was purified by flash chromatography on silica gel (DCM/*n*-Pentane 3:2) giving **12a** as a dark yellow solid (7 mg, 33% yield). **mp** >300°C. **^{1}H NMR (500 MHz, $CDCl_3$):** δ 14.53 (s, 1H), 8.83 (s, 1H), 8.43-8.38 (m, 2H), 8.35 (s, 1H), 8.14-8.10 (m, 1H), 7.92-7.89 (m, 1H), 7.87-7.84 (m, 2H). **^{13}C {H} NMR (126 MHz, $CDCl_3$):** δ 188.1, 182.3, 163.7, 137.9, 135.0, 134.6, 134.5, 134.0, 131.3, 130.56, 130.55 (q, $^2J_{C-F}$ = 33.4 Hz), 127.9, 127.3, 127.2, 126.9 (q, $^3J_{C-F}$ = 3.0 Hz), 123.9 (q, $^1J_{C-F}$ = 272.6 Hz), 122.7 (q, $^3J_{C-F}$ = 4.5 Hz), 120.8, 110.5. **^{19}F NMR (471 MHz, $CDCl_3$):** δ -62.66. **HRMS (ESI-)** *m/z*: $[M-H]^-$ calculated for $C_{19}H_8F_3O_3$: 341.0431, found 341.0430.

6-hydroxy-8-(trifluoromethyl)tetracene-5,12-dione (12b). To a stirred solution of 6,11-dimethoxy-2-(trifluoromethyl)tetracene-5(12H)-one **10b** (72 mg, 0.19 mmol, 1.0 equiv.) and TBAI (0.14 g, 0.39 mmol, 2.0 equiv.) in dry DCM under argon atmosphere was added dropwise BCl_3 (0.58 mL, 0.58 mmol, 3.0 equiv.) at -78 °C. The reaction mixture was allowed to warm up slowly to room temperature and stirred 16 h (CCM, SiO_2, DCM/*n*-Pentane 1:1). The reaction mixture was quenched with saturated aqueous solution of Na_2CO_3 (2 x 10 mL) and the organic phase was separated. The aqueous phase was further extracted with DCM (3 x 10 mL). The combined organic phases were washed with water (3 x 10 mL) and brine (3 x 10 mL) then dried over $MgSO_4$, filtered, and evaporated under reduced pressure. Chromatography on silica gel with DCM (20 to 50%) in *n*-Pentane afforded the title compound **12b** as a brown solid (26 mg, 40%). **mp** >300°C. **^{1}H NMR (500 MHz, $CDCl_3$):** δ 14.18 (s, 1H), 8.68-8.65 (m, 1H), 8.43-8.38 (m, 3H), 8.29 (s, 1H), 7.88-7.85 (m, 3H). **^{13}C {H} NMR (126 MHz, $CDCl_3$):** δ 188.2, 182.1, 162.9, 135.6, 134.9, 134.5 (2*C*), 133.9, 132.6 (d, $^2J_{C,F}$ = 33.5 Hz), 129.8, 129.4, 127.8, 127.5 (q, $^3J_{C,F}$ = 3.8 Hz), 127.2, 126.1, 124.4 (q, $^3J_{C,F}$ = 3.8 Hz), 123.6 (d, $^1J_{C,F}$ = 272.9 Hz), 121.6, 110.8. **^{19}F NMR (471 MHz, $CDCl_3$):** δ -63.00. **HRMS (ESI-)** *m/z*: $[M-H]^-$ calculated for $C_{19}H_8F_3O_3$: 341.0431, found 341.0446.

3,3'-(ethane-1,2-diyl)bis(2-(4-(trifluoromethyl)benzoyl)naphthalene-1,4-dione), PDO-dimer (13). A solution of 2-(fluoromethyl)-3-(4-(trifluoromethyl)benzoyl)naphthalene-1,4-dione **F-PDO**, (100 mg, 0.28 mmol, 1.0 equiv.) in a mixture of ^{i}PrOH and DCM (2 mL, 1:1, v/v) was stirred whilst irradiated

under UV light for 24 h at 16 °C under argon. After this time, the solvent was evaporated and the crude residue was purified by flash chromatography on silica gel using toluene 100% as eluent giving **13** as a dark orange solid (77 mg, 41% yield). **mp** decomposes at approximately 250°C. **^{1}H NMR (400 MHz, $CDCl_3$):** δ 8.11-8.05 (m, 2H), 8.04-7.99 (m, 2H), 7.92-7.87 (m, 4H), 7.83-7.76 (m, 4H), 7.63-7.55 (m, 4H), 2.77 (s, 4H). **^{13}C NMR (101 MHz, $CDCl_3$):** δ 192.8 (2C), 184.4 (2C), 183.8 (2C), 146.2 (2C), 144.5 (2C), 138.4 (2C), 135.5 (q, $^{2}J_{C\text{-}F}$ = 33.0 Hz, 2C), 134.6 (2C), 134.4 (2C), 132.1 (2C), 131.3 (2C), 129.6 (4C), 126.8 (2C), 126.6 (2C), 126.1 (q, $^{3}J_{C\text{-}F}$ = 3.8 Hz, 4C), 123.4 (q, $^{1}J_{C\text{-}F}$ = 273.1 Hz, 2C), 27.2 (2C). **^{19}F NMR (376 MHz, $CDCl_3$):** δ -63.2 (6F). **HRMS (ESI+)** *m/z*: $[M+Na]^+$ calculated for $C_{38}H_{20}F_6O_6$: 709.1062, found 709.1067.

Data Availability Statement

The data underlying this study are available in the published article and its Supporting Information

Supporting Information

The Supporting Information is available free of charge at https://pubs.acs.org/doi/xxxxxxxxxxxxx.

Procedures and additional data: methods for the synthesis and physicochemical analyses used to study the investigated compounds, NMR data of new compounds, absorption, emission and ESI-HRMS data of UV-irradiated systems, electrochemical data for major investigated compounds, spectrophotometric data for major investigated compounds with biological relevant derivatives and models.

Author Information

Corresponding Author

* E-mail: elhabiri@unistra.fr

Notes

The authors declare no competing financial interest.

Acknowledgments

This work was supported by the Université de Strasbourg and the CNRS. The authors wish to thank the Laboratoire d'Excellence (LabEx) ParaFrap consortium for funding [ANR-11-LABX-0024], and creating a proper framework for this scientific research. This observation of metabolite fluorescence, discovered by serendipity, has also benefited from the received financial support from the CNRS through the MITI interdisciplinary programs "Vie & lumière". Dr Valérie Mazan (LIMA UMR7042) is gratefully acknowledged for the quantum yield measurements.

References

1 a) Singh, M. S.; Nagaraju, A.; Anand, N.; Chowdhury, S. Ortho-Quinone Methide (o-QM): A Highly Reactive, Ephemeral and Versatile Intermediate in Organic Synthesis. *RSC Adv.* **2014**, *4(99)*, 55924-55959. b) Arumugam, S.; Popik, V. V. Photochemical Generation and the Reactivity of *o* -Naphthoquinone Methides in Aqueous Solutions. *J. Am. Chem. Soc.* **2009**, *131(33)*, 11892-11899.

2 Bai, W.-J.; David, J. G.; Feng, Z.-G.; Weaver, M. G.; Wu, K.-L.; Pettus, T. R. R. The Domestication of *Ortho* -Quinone Methides. *Acc. Chem. Res.* **2014**, *47(12)*, 3655–3664.

3 Meier, H. Benzoxetes and Benzothietes - Heterocyclic Analogues of Benzocyclobutene. *Molecules* **2012**, *17(2)*, 1548-1570.

4 Pettus, T. R. R.; Selenski, C. Product Subclass 1: o-Quinomethanes. In Science of Synthesis, Compounds with Two Carbon-heteroatom Bonds, Griesbeck, A. G., Thieme Publishing Group, **2006**, 831-872.

[5] Van De Water, R. W.; Pettus, T. R. R. O-Quinone Methides: Intermediates Underdeveloped and Underutilized in Organic Synthesis. *Tetrahedron* **2002**, *58(27)*, 5367-5405.

[6] Toteva, M. M.; Richard, J. P. The Generation and Reactions of Quinone Methides. In *Advances in Physical Organic Chemistry*; Elsevier, **2011**, *45*, 39-91.

[7] Thomson, R. H.; Worthington, R. D. Quinones. Part 9. l Side-Chain Alkylthiolation of Methyl-1,4-Naphtho-Quinones. *J. Chem. Soc., Perkin Trans. 1* **1980**, 282-288.

[8] Thomson, R. H.; Worthington, R. D. Part 10. I. Side-Chain Methylthiolation of Methylbenzo-Quinones. *J. Chem. Soc., Perkin Trans. 1* **1980**, 289-292.

[9] Chandrasenan, K.; Thomson, R.H. Biquinones-III. The Dimerisation of 1,4-Naphthaquinones, *Tetrahedron* **1971**, *27*, 2529-2539

[10] Laatsch, H. Dimere Naphthochinone, V. 3′,4′-Dihydro-4,6′-dimethoxyspiro[naphthalin-2(1*H*),2′-[2*H*]-naphtho[1,2-*b*]pyran]-1-on; Bildung und Thermolyseprodukte eines ungewöhnlichen Spirochinolethers. *Liebigs Ann. Chem.* **1982**, 1808-1828.

[11] Onuki, M.; Ota, M.; Otokozawa, S.; Kamo, S.; Tomoshige, S.; Tsubaki, K.; Kuramochi, K. Dimerizations of 2-Bromo-3-Methyl-1,4-Naphthoquinone and 2-Methyl-1,4-Naphthoquinone in Tetra-n-Butylammonium Bromide. *Tetrahedron* **2020**, *76(6)*, 130899.

[12] a) Antonini, I.; Lin, T. S.; Cosby, L. A.; Dai, Y. R.; Sartorelli, A. C. 2- and 6-Methyl-1,4-Naphthoquinone Derivatives as Potential Bioreductive Alkylating Agents. *J. Med. Chem.* **1982**, *25* (6), 730–735. b) Lin, A. J.; Sartorelli, Alan C. Potential bioreductive alkylating agents. VI. Determination of the Relationship between Oxidation-Reduction Potential and Antineoplastic Activity. *Biochem. Pharmacol.* **1976**, *25(2)*, 206-207. c) Chatterjee, M.; Rokita, S. E. The Role of a Quinone Methide in the Sequence Specific Alkylation of DNA. *J. Am. Chem. Soc.* **1994**, *116(5)*, 1690-1697.

[13] Bauer, H.; Fritz-Wolf, K.; Winzer, A.; Kühner, S.; Little, S.; Yardley, V.; Vezin, H.; Palfey, B.; Schirmer, R. H.; Davioud-Charvet, E. A Fluoro Analogue of the Menadione Derivative 6-[2′-(3′-Methyl)-1′,4′-Naphthoquinolyl]Hexanoic Acid Is a Suicide Substrate of Glutathione Reductase. Crystal Structure of the Alkylated Human Enzyme. *J. Am. Chem. Soc.* **2006**, *128(33)*, 10784-10794.

[14] Swartz, A. M.; Patton, V.; Heppleston, M. J.; Barra, M. On the Photoreactivity of Vitamin K Compounds. *Int. J. Chem. Kinet.* **2008**, *40(12)*, 839–844.

[15] a) Creed, D.; Werbin, H.; Daniel, T. The Mechanism of Photooxidation of the Menaquinones. *Tetrahedron Letters* **1981**, *22(22)*, 2039-2042. b) Hangarter, M.-A.; Hörmann, A.; Kamdzhilov, Y.; Wirz, J. Primary Photoreactions of Phylloquinone (Vitamin K1) and Plastoquinone-1 in Solution. *Photochem Photobiol Sci* **2003**, *2(5)*, 524-535. c) Leary, G.; Porter, G. The Photochemistry of Two Phytyl Quinones: A-Tocopherylquinone and Vitamin K1. *J. Chem. Soc. A: Inorg. Phys. Theor.* **1970**, 2273-2278.

[16] a) Khdour, O.; Skibo, E. B. Quinone Methide Chemistry of Prekinamycins: 13C- Labeling, Spectral Global Fitting and in Vitro Studies. *Org. Biomol. Chem.* **2009**, *7(10)*, 2140-2154. b) Feldman, K. S.; Eastman, K. J. Studies on the Mechanism of Action of Prekinamycin, a Member of the Diazoparaquinone Family of Natural Products: Evidence for Both Sp^2 Radical and Orthoquinonemethide Intermediates. *J. Am. Chem. Soc.* **2006**, *128(38)*, 12562-12573.

[17] Cichocki, B.A.; Donzel, M.; Heimsch, K.C.; Lesanavičius, M.; Feng, L.; Montagut, E.J.; Becker, K.; Aliverti, A.; Elhabiri, M.; Cenas, N.; Davioud-Charvet, E. *Plasmodium falciparum* ferredoxin-NADP(+) reductase-catalyzed redox cycling of plasmodione generates both predicted key drug metabolites. Implication for antimalarial drug development. *ACS Inf. Dis.* **2021**, *7(7)*, 1996-2012

[18] Gerber, E.; Hemmerlin, A.; Hartmann, M.; Heintz, D.; Hartmann, M.-A.; Mutterer, J.; Rodríguez-Concepción, M.; Boronat, A.; Van Dorsselaer, A.; Rohmer, M.; Crowell, D. N.; Bach, T. J. The Plastidial 2-*C*-Methyl-d-Erythritol 4-Phosphate Pathway Provides the Isoprenyl Moiety for Protein Geranylgeranylation in Tobacco BY-2 Cells. *Plant Cell* **2009**, *21(1)*, 285-300.

[19] Chevalier, Q.; Gallé, J.-B.; Wasser, N.; Mazan, V.; Villette, C.; Mutterer, J.; Elustondo, M. M.; Girard, N.; Elhabiri, M.; Schaller, H.; Hemmerlin, A.; Vonthron-Sénécheau, C. Unravelling the Puzzle of Anthranoid Metabolism in Living Plant Cells Using Spectral Imaging Coupled to Mass Spectrometry. *Metabolites* **2021**, *11(9)*, 571.

[20] Friebolin, W.; Jannack, B.; Wenzel, N.; Furrer, J.; Oeser, T.; Sanchez, C. P.; Lanzer, M.; Yardley, V.; Becker, K.; Davioud-Charvet, E. Antimalarial Dual Drugs Based on Potent Inhibitors of Glutathione Reductase from Plasmodium Falciparum. *J. Med. Chem.* **2008**, *51(5)*, 1260-1277.

[21] Anderson, J. M.; Kochi, J. K. Silver(I)-Catalyzed Oxidative Decarboxylation of Acids by Peroxydisulfate. Role of Silver(II). *J. Am. Chem. Soc.* **1970**, *92(6)*, 1651-1659.

[22] Natori, K.; Iwayama, T.; Yamabe, O.; Kitamoto, Y.; Ikeda, H.; Sakamoto, K.; Hattori, T.; Miyano, S. Photoracemization of Blestriarene C and Its Analogs. *Chirality* **2015**, *27* (8), 479-486.

[23] Cotos, L.; Donzel, M.; Elhabiri, M.; Davioud-Charvet, E. A Mild and Versatile Friedel–Crafts Methodology for the Diversity-Oriented Synthesis of Redox-Active 3-Benzoylmenadiones with Tunable Redox Potentials. *Chem. Eur. J.* **2020**, *26(15)*, 3314-3325.

[24] Brooks, P. R.; Wirtz, M. C.; Vetelino, M. G.; Rescek, D. M.; Woodworth, G. F.; Morgan, B. P.; Coe, J. W. Boron Trichloride/Tetra-n-Butylammonium Iodide: A Mild, Selective Combination Reagent for the Cleavage of Primary Alkyl Aryl Ethers. *J. Org. Chem.* **1999**, *64* (26), 9719-9721.

[25] a) Brand, D. J.; Fisher, J. Tautomeric Instability of 10-Deoxydaunomycinone Hydroquinone. *J. Am. Chem. Soc.* **1986**, *108* (11), 3088-3096. b) Schweitzer, B. A.; Koch, T. H. Synthesis and Redox Chemistry of 5-Deoxydaunomycin. A Long-Lived Hydroquinone Tautomer. *J. Am. Chem. Soc.* **1993**, *115* (13), 5440-5445.

[26] Feng L, Lanfranchi DA, Cotos L, Cesar-Rodo E, Ehrhardt K, Goetz AA, Zimmermann H, Fenaille F, Blandin SA, Davioud-Charvet E. Synthesis of plasmodione metabolites and ^{13}C-enriched plasmodione as chemical tools for drug metabolism investigation. Org. Biomol. Chem. **2018**, *16(15*), 2647-2665.

[27] Elhabiri, M.; Sidorov, P.; Cesar Rodo, E.; Marcou, G.; Lanfranchi, D. A.; Davioud-Charvet, E.; Horvath, D.; Varnek, A. Electrochemical Properties of Substituted 2-Methyl-1,4-Naphthoquinones: Redox Behavior Predictions. *Chem. Eur. J.* **2015**, *21*, 3415-3424.

[28] Sidorov, P.; Desta, I.; Chessé, M.; Horvath, D.; Marcou, G.; Varnek, A.; Davioud-Charvet, E.; Elhabiri, M. Redox Polypharmacology is an Emerging Strategy to Combat Malarial Parasites. *ChemMedChem* **2016**, *11*, 1339-1351.

[29] Bielitza, M.; Belorgey, D.; Ehrhardt, K.; Johann, L.; Lanfranchi, D.A.; Gallo, V.; Schwarzer, E.; Mohring, F.; Jortzik, E.; Williams, D.L.; Becker, K.; Arese, P.; Elhabiri, M.; Davioud-Charvet, E. Antimalarial NADPH-Consuming Redox-Cyclers as Superior G6PD Deficiency Copycats. *Antiox. Red. Signal.* **2015**, *22*, 1337-1351.

[30] Gaudiano, G.; Frigerio, M.; Bravo, P.; Koch, T. H. Reduction of Daunomycin in Dimethyl Sulfoxide. Long-Lived Semiquinones and Quinone Methide and Formation of an Enolate at the 14-Position via the Quinone Methide. *J. Am. Chem. Soc.* **1992**, *114(8)*, 3107-3113.

[31] Shaikh, A. kadar; Cobb, A. J. A.; Varvounis, G. Mild and Rapid Method for the Generation of *Ortho* -(Naphtho)Quinone Methide Intermediates. *Org. Lett.* **2012**, *14(2)*, 584-587.

[32] Cavitt, S. B.; R., H. S.; Gardner, P. D. The Structure of O-Quinone Methide Trimer. *J. Org. Chem.* **1962**, *27(4)*, 1211-1216.

[33] Lanfranchi, D. A.; Belorgey, D.; Müller, T.; Vezin, H.; Lanzer, M.; Davioud-Charvet, E. Exploring the Trifluoromenadione Core as a Template to Design Antimalarial Redox-Active Agents Interacting with Glutathione Reductase. *Org. Biomol. Chem.* **2012**, *10(24)*, 4795-4806.

[34] Wayner, D. D. M.; McPhee, D. J.; Griller, D. Oxidation and Reduction Potentials of Transient Free Radicals. *J. Am. Chem. Soc.* **1988**, *110(1)*, 132-137.

[35] Hünig, S.; Bau, R.; Kemmer, M.; Meixner, H.; Metzenthin, T.; Peters, K.; Sinzger, K.; Gulbis, J. 2,5-DisubstitutedN, N′-Dicyanoquinone Diimines (DCNQIs) − Syntheses and Redox Properties. *Eur. J. Org. Chem.* **1998**, *1998(2)*, 335-348.

[36] Cook, C. D.; Butler, L. C. Dimerization of the Quinone Methide, 2,4-Di-Tert-Butyl-6-Ethylidene-2,5-Cyclohexadien-1-One. Possible Diels-Alder Mechanism. *J. Org. Chem.* **1969**, *34(1)*, 227-229.

[37] Ezcurra, J. E.; Karabelas, K.; Moore, H. W. Formation of Reactive O-Quinone Methides from the Reaction of Trimethylsilyl(Methyl)-Substituted 1,4-Benzoquinones with Nucleophiles. *Tetrahedron* **2005**, *61(1)*, 275-286.

[38] Jurd, L. Quinones and quinone-methides—I : Cyclization and dimerisation of crystalline ortho-quinone methides from phenol oxidation reactions. *Tetrahedron* **1977**, *33*, 163-168.

[39] Leo, E. A.; Delgado, J.; Domingo, L. R.; Espinós, A.; Miranda, M. A.; Tormos, R. Photogeneration of *o* -Quinone Methides from *o* -Cycloalkenylphenols. *J. Org. Chem.* **2003***, 68(25)*, 9643-9647.

[40] Osyanin, V. A.; Lukashenko, A. V.; Osipov, D. V. Cycloaddition Reactions of O-Quinone Methides with Polarized Olefins. *Russ. Chem. Rev.* **2021**, *90(3)*, 324–373.

[41] Dean, F. M.; Houghton, L. E.; Morton, R. B. Adducts from Quinones and Diazoalkanes. Part VII. The Function of Quinone Methides in the Side-Chain Amination of Alkylquinones and in Dimerisations Giving Ethylenediquinones. *J. Chem. Soc. C: Org.* **1968**, 2065-2069.

[42] Davioud-Charvet, E.; Lanfranchi, D. A. Subversive Substrates of Glutathione Reductases from *Plasmodium Falciparum* -Infected Red Blood Cells as Antimalarial Agents. In *Apicomplexan Parasites*; Becker, K., Ed.; Wiley, **2011**, 373-396.

[43] Görner, H. Photoreactions of 2-Methyl-5-Isopropyl-1,4-Benzoquinone. *J. Photochem. Photobiol. A: Chem.* **2004**, *165(1–3)*, 215-222.

[44] Poulsen, J. R.; Birks, J. W. Photoreduction Fluorescence Detection of Quinones in High-Performance Liquid Chromatography. *Anal. Chem.* **1989**, *61(20)*, 2267-2276.

[45] Donzel, M.; Elhabiri, M.; Davioud-Charvet, E. A bioinspired photoredox benzylation of quinones catalyzed by iron(III). *J. Org. Chem.* **2021**, *86(15)*, 10055-10066.

[46] Görner, H. Photoprocesses of P-Naphthoquinones and Vitamin K1: Effects of Alcohols and Amines on the Reactivity in Solution. *Photochem Photobiol Sci* **2004**, *3(1)*, 71-78.

[47] a) Keire, D. A.; Strauss, E.; Guo, W.; Noszal, B.; Rabenstein, D. L. Kinetics and Equilibria of Thiol/Disulfide Interchange Reactions of Selected Biological Thiols and Related Molecules with Oxidized Glutathione. *J. Org. Chem.* **1992**, *57* (1), 123–127. b) Lukesh, J. C.; Palte, M. J.; Raines, R. T. A Potent, Versatile Disulfide-Reducing Agent from Aspartic Acid. *J. Am. Chem. Soc.* **2012**, *134(9)*, 4057-4059.

[48] Turell, L.; Carballal, S.; Botti, H.; Radi, R.; Alvarez, B. Oxidation of the Albumin Thiol to Sulfenic Acid and Its Implications in the Intravascular Compartment. *Braz. J. Med. Biol. Res.* **2009**, *42(4)*, 305-311.

[49] Müller, T.; Johann, L.; Jannack, B.; Brückner, M.; Lanfranchi, D. A.; Bauer, H.; Sanchez, C.; Yardley, V.; Deregnaucourt, C.; Schrével, J.; Lanzer, M.; Schirmer, R. H.; Davioud-Charvet, E. Glutathione Reductase-Catalyzed Cascade of Redox Reactions To Bioactivate Potent Antimalarial 1,4-Naphthoquinones – A New Strategy to Combat Malarial Parasites. *J. Am. Chem. Soc.* **2011**, *133(30)*, 11557-11571.

[50] a) Di Monte, D.; Ross, D.; Bellomo, G.; Eklöw, L.; Orrenius, S. Alterations in Intracellular Thiol Homeostasis during the Metabolism of Menadione by Isolated Rat Hepatocytes. *Arch. Biochem. Biophys*. **1984**, *235(2)*, 334-342. b) Nickerson, W. J.; Falcone, G.; Strauss, G. Studies on Quinone-Thioethers. I. Mechanism of Formation and Properties of Thiodione. *Biochemistry* **1963**, *2(3)*, 537-543.

[51] Scott, G. K.; Atsriku, C.; Kaminker, P.; Held, J.; Gibson, B.; Baldwin, M. A.; Benz, C. C. Vitamin K3 (Menadione)-Induced Oncosis Associated with Keratin 8 Phosphorylation and Histone H3 Arylation. *Mol. Pharmacol.* **2005**, *68(3)*, 606-615.

[52] Spruit, C. J. P. Absorption Spectra of Quinones. I. Naphthoquinones and Naphthohydroquinones. *Recl. Trav. Chim. Pays-Bas* **2010**, *68(4)*, 309-324.

[53] Nagar, B.; Dhar, B. B. Visible Light-Mediated Thiolation of Substituted 1,4-Naphthoquinones Using Eosin Y as a Photoredox Catalyst. *J. Org. Chem.* **2022**, *87(5)*, 3195-3201.

[54] Jha, R. K.; Upadhyay, A.; Kanika; Jain, S.; K A, N.; Kumar, S. Light-Driven Carbon–Carbon Coupling of α-Sp^3–CH of Aliphatic Alcohols with Sp^2–CH Bond of 1,4-Naphthoquinones. *Org. Lett.* **2022**, *24(41)*, 7605-7610.

[55] Brimble, M. A.; Laita, O.; Robinson, J. E. Addition of 2-Tert-Butyldimethylsilyloxythiophene to Activated Quinones: An Approach to Thia Analogues of Kalafungin. *Tetrahedron* **2006**, *62(13)*, 3021-3027.

[56] Sharma , A. K.; Jain, V. K.; Machwe, M. K.; Zaidi, Z. H. Fluorescence Characteristics of Some Hydroxyl-Substituted Naphthalenes. *Can. J. Appl. Spectro.* **1992**, *37*, 6-9.

[57] Shie, T.-L.; Lin, C.-H.; Lin, S.-L.; Yang, D.-Y. Synthesis of 1,1,3-Trisubstituted Naphtho[2,3-c]pyran-5,10-dione Derivatives as Potential Redox Switches. *Eur. J. Org. Chem.* **2007**, 4831-4836

[58] a) Sedgwick, A. C.; Wu, L.; Han, H.-H.; Bull, S. D.; He, X.-P.; James, T. D.; Sessler, J. L.; Tang, B. Z.; Tian, H.; Yoon, J. Excited-State Intramolecular Proton-Transfer (ESIPT) Based Fluorescence Sensors and Imaging Agents. *Chem. Soc. Rev.* **2018**, *47(23)*, 8842-8880. b) Joshi, H. C.; Antonov, L. Excited-State Intramolecular Proton Transfer: A Short Introductory Review. *Molecules* **2021**, *26(5)*, 1475.

[59] Gashnga, P. M.; Singh, T. S.; Mitra, S. Modulation of ESIPT Fluorescence in O-Hydroxy Acetophenone Derivatives: A Comparative Study in Different Bio-Mimicking Aqueous Interfaces. *J. Mol. Liquids* **2016**, *218*, 549-557.

[60] Han, C.; Song, B.; Liang, X.; Pan, H.; Dong, W. Design and Application of a Fluorescent Probe Based on ESIPT Mechanism for the Detection of Cys with *o* -Hydroxyacetophenone Structure. *Anal. Methods* **2019**, *11(19)*, 2513-2517.

[61] Tarzi, O. I.; Stéfano, L. D.; Argüello, J. E.; Oksdath-Mansilla, G.; Erra-Balsells, R. Photochemical and Thermal Stability of Some Dihydroxyacetophenones Used as UV-MALDI-MS Matrices. *Photochem. Photobiol.* **2013**, *89(6)*, 1368-1374.

[62] Catalán, J.; Del Valle, J. C.; Díaz, C.; Palomar, J.; De Paz, J. L. G.; Kasha, M. Solvatochromism of Fluorophores with an Intramolecular Hydrogen Bond and Their Use as Probes in Biomolecular Cavity Sites. *Int. J. Quant. Chem.* **1999**, *72(4)*, 421-438.

[63] Sayed, M.; Balayan, J.; Singh, P. K.; Pal, H. Modulation of Excited-State Photodynamics of ESIPT Probe 1'-Hydroxy-2'-Acetonaphthone (HAN) on Interaction with Bovine Serum Albumin. *J. Photochem. Photobiol. A: Chem.* **2020**, *400*, 112651.

[64] Ning, C.; Xiao, C.; Lu, R.; Zhou, P. Whether the Excited State Intramolecular Proton Transfer of 1-Hydroxy-2-Acetonaphthone Will Happen? *J. Lumin.* **2020**, *217*, 116825.

[65] Tobita, S.; Yamamoto, M.; Kurahayashi, N.; Tsukagoshi, R.; Nakamura, Y.; Shizuka, H. Effects of Electronic Structures on the Excited-State Intramolecular Proton Transfer of 1-Hydroxy-2-Acetonaphthone and Related Compounds. *J. Phys. Chem. A* **1998**, *102(27)*, 5206-5214.

[66] Wilson, R. M.; Hannemann, K.; Peters, K.; Peters, E. M. Conventional and Laser-Jet Photochemistry of 2-Methylbenzophenone. *J. Am. Chem. Soc.* **1987**, *109(15)*, 4741-4743.

[67] Terenzi, A.; La Franca, M.; van Schoonhoven, S.; Panchuk, R.; Martínez, Á.; Heffeter, P.; Gober, R.; Pirker, C.; Vician, P.; Kowol, C. R.; Stoika, R.; Salassa, L.; Rohr, J.; Berger, W. Landomycins as Glutathione-Depleting Agents and Natural Fluorescent Probes for Cellular Michael Adduct-Dependent Quinone Metabolism. *Commun. Chem.* **2021**, *4(1)*, 162.